The spread and persistence of Rabies in the Arctic:

a modeling study

By

© E. Joe Moran

A thesis submitted to the School of Graduate Studies in partial fulfillment of the requirements for the degree of

Master of Science

Department of Biology

Memorial University of Newfoundland

April 2020

St. John’s Newfoundland and Labrador

Acknowledgements

First and foremost, I would like to thank my advisors, Dr. Amy Hurford and Dr. Nicolas Lecomte. Amy, I have learned more from you than perhaps anyone I've ever met on my path through academia. Your careful explanations and vast knowledge are gifts to anyone willing to learn, and our weekly meetings provided the motivation I needed to complete this research. Nic, I can't thank you enough for our conversations about arctic rabies and the biological realism that you helped bring to our research. A special thanks also goes out to Dr. Patrick Leighton, who has given me excellent feedback and has contributed to the foundational ideas in this paper. I would like to thank the Hurford Lab: Joany, Abdou, Fabio, and Joey –you guys were always there to help and talk when I needed a reprieve from my work, and you made my time at MUN unforgettable. Lastly, I would like to thank the Leroux Lab for cookies, chocolate, and fun breaks from our work.

Table of Contents

List of Tables

List of Figures

Figure 3.3: When climate warming occurs, lagging northern infecteds "bridge the gap" between previously isolated populations, allowing disease to be transmitted to the uninfected southern population. (a) Prior to climate warming (t=199), the densities of southern susceptibles (solid red line) and northern infecteds (blue dotted line) do not overlap, in part due to the different thermal niches for each population (red and blue dash-dotted lines). (b) After 25 years of continuous climate warming (t=225), the thermal niches of both populations have moved northwards (red and blue dashed-dotted lines), as have the population densities, although southern susceptibles (red solid line) and northern infecteds (blue solid line) both lag to the south of their northern thermal tolerance limits (right-most dashed-dotted lines). The lag of the northern infected population (blue dotted line) behind its southern thermal tolerance limit (left-most blue dashed-dotted line) is sufficient to "bridge the gap" to the northern limit of the southern susceptible population (right-most red solid line). The infected northern individuals (blue dashed line) shown south of x = 40 occupy habitat that is too warm at t=225 years (b), and will ultimately go extinct even if no further climate warming occurs, but extinction takes time and disease spread to the southern population is enabled via this transient persistence. Parameters are as for Figure 3.2 and the density of northern susceptibles and southern infected are not shown to clearly visualize the gap between northern infected and southern susceptibles……61

Figure A.1: Very low landscape level averages $\overline{K}$=0.7 fox/km^2 (a) and $\overline{K}$=0.5 fox/km^2 (b) provide limited parameter space for endemicity (a) and can be exhausted of its disease by dispersal without effectively infecting the other patch (b). $\overline{K} = (K_1 + K_2)/2$, is taken across the two patches in the landscape. The landscape-level prevalence (%) of rabies, is for ascending values of the low-carrying capacity patch 1, and the carrying capacity on patch 2 is $2\overline{K} - K_1$. When $K_1 = K_2 = \overline{K}/2 < K_T$, no disease occurs on either patch, however, as the variance in the K_i between the two patches increases, rabies becomes established on both patches in (a), although at extremely low prevalence. Dispersal is unidirectional with m_{12}=0 and m_{21}=0.1. Unless otherwise stated, all parameter values are as given in Table 2.1…….....79

Chapter 1: General Introduction

Rabies is a neurodegenerative virus in the lyssavirus genus. The first written accounts of rabies come from the Babylonian Empire between 2000 and 3000 b.c.e, where the possession of an infected dog was an offense that warranted a large paid fine (Wasik 2013). Approximately 5000 years later, and despite a plentitude of management and research, rabies persists on 6 of 7 continents, contributing to approximately 60,000 deaths per year, in addition to the 15 million successful post bite vaccinations given annually (World Health Organization 2015). Rabies is a unique virus, given its high virulence and disease-induced behavioral modulations, both of which help the virus propagate itself through wildlife populations and facilitate zoonotic spillovers. Rabies' ill effects has rendered it an iconic disease that has inspired vast amounts of epidemiological research and has brought about some of the most coordinated and successful disease control regimes for both wildlife and domestic animals.

Transmission of the virus generally occurs via a bite wound from an infected animal. After a victim has been infected, a latent stage occurs while the virus replicates at the bite wound and ascends the peripheral nervous system, which can take days to months. Once the virus reaches the central nervous system, clinical symptoms such as fever, aches, hydrophobia, paralysis, delirium, aggression, paranoia, and coma begin to occur. At the onset of clinical symptoms, the host has several days to a month to live. The virus nearly always ends with fatal encephalitis. To date, fewer than 20 humans have survived the disease, and in rare strains of rabies in arctic fox and African hyenas, there are low rates of recovery (Ballard et al. 2001, de Souza and Madhusudana 2014, East et al. 2001).

Arctic Rabies is maintained by two host species, the arctic and red fox. As a widespread generalist, red foxes inhabit temperate regions up to and including portions of the Arctic circle. Overlap occurs with arctic fox from the northern portion of central Canadian provinces up to, and including, portions of the Arctic circle, thereafter, arctic foxes are the sole inhabitant (MacPherson 1964, Monchot and Grendon 2010). Red fox's northern range is governed by a threshold in metabolic maintenance given colder temperatures and lower productivity for generalist predators, while the southern boundary of the arctic fox's range is limited by interspecific competition with red fox (Hersteinsson and MacDonald 1992).

Arctic rabies is unique in that the disease remains endemic at very low prevalence values (< 1%) with low host densities (< 0.3 breeders/km^2) in a discontinuous landscape (Angerbjörn et al. 1999, Mork et al. 2011). One fox per square kilometer is widely regarded as the density threshold for rabies disease persistence in a homogenous landscape, which is derived in Anderson et al. (1981). Arctic rabies, however, remains endemic, potentially due to spatial heterogeneity in resource abundance, where some local areas have carrying capacities that exceed the threshold. These areas are towns, prairie potholes, coastlines, and migration corridors, all of which theoretically provide regions where rabies can be endemically infected (Harris 1981, Savory et al. 2014, Trewhella et al. 1988). In addition to spatially heterogenous resource distribution, the Arctic is defined by its spatial discontinuity, where discrete patches can be the Northwest Territories, Nunavut, Greenland, and Svalbard, and their associated islands.

The assumptions of metapopulation theory fit well with the defining features of the Arctic—spatial discontinuity and heterogenous distribution of resources. Models that account for these spatial features can allow for diseases persistence as individual populations can be "rescued" by incoming disease, thus preventing a disease extirpation that would have subsequently occurred in an equivalent homogenous environment (Bolker and Grenfell 1995, Hagenaars et al. 2004, Schwartz et al. 1992, Wang and Zhao 2004). Metapopulation theory allows diseases to persist when at least one of the subpopulations can support the disease independently, assuming mass action transmission for intrapatch infections (Hethcote 1976). This can be exemplified in a two-patch model, where one patch is endemically infected and the other is not, in which disease can die out of the system, or persists in both patches, given the level of dispersal amongst them (Wang and Zhao 2004). Although connectivity always decreases the R_0 of a metapopulation system with source and sink patches, which is also in accordance with Hethcote (1976); low levels of dispersal can increase prevalence in the system (Gurarie et al. 2008). Without spatially structured source-sink disease dynamics, rescue effects, and reintroductions, disease dynamics become an average of all interactions, and are not partitioned in a biologically representative scheme.

Climate change shifts species ranges, facilitates disease spread, and amplifies disease incidence (Bellard et al. 2012, Chen et al. 2011, Patz et al. 1996, Thuiller 2007); having notable effects on diseases such as malaria (Martens et al. 1996), dengue fever (Hales et al. 2002), bluetongue (Purse et al. 2005), chytrid fungus (Pounds 2001), wooly adelgid beetle in hemlocks (Paradis et al. 2008), beech bark disease (Stephanson et al.

2017), and lyme disease (Brownstein et al. 2005). To explore how climate change alters disease systems, such as those previously stated, mathematical models have been used to understand the climate, host, and disease relationships. This can be done by using ecological niche modeling, metabolic theory of ecology, host-parasite or host-parasite-vector dynamics, suitability models, and population models with temperature dependent survival or fecundity (Altizer et al. 2013, Brownstein et al. 2005, Molnar et al. 2013, Peterson et al. 2006, Urban et al. 2013). For climate change models to effectively characterize disease in a changing world, they must account for warming temperatures, shifting ranges, perturbed food webs and species interactions, transient dynamics, metabolic tolerances, and other temperature dependent constraints. Unlike rabies, many of the previously stated diseases have temperature-dependent vectors or pathogens and will necessarily shift with a warming climate. It is less clear how rabies will be affected by climate change as there are hosts found at nearly every latitude, and while hosts species densities may be affected by climate warming, other aspects of the transmission dynamics are relatively unaffected by temperature. To understand how climate warming might affect rabies dynamics, we use a moving habitat model. Moving habitat models have been previously used to study a species' ability to track climate change, how the speed of climate change impacts population dynamics, and how a populations' profile responds to a shifting habitat (Berestyki et al. 2009, Hurford et al. 2019, Potapov and Lewis 2004). We present one of the few studies that uses moving habitat models to understand disease dynamics, and possibly the first study to use this technique with a multi-species epidemiological system.

The isolated nature of endemically infected northern regions makes studying arctic rabies difficult. With a lack of epidemiological studies of arctic rabies, we take this opportunity to explore arctic rabies via mathematical modeling. By using models, we can incorporate existing data and knowledge to inform the structure of our models and the assumptions they make. This allows us to simulate a variety of scenarios for lengths of time that would not be feasible in controlled experiments. By adopting this methodology, we can investigate driving mechanisms of the disease and predict future dynamics, something other methodological techniques would not allow for.

We derive two mathematical models to understand rabies in the Arctic. Chapter two uses a two-patch metapopulation model, where patches represent different levels of resource abundance. This model allows us to explore the effect of spatial heterogeneity on the persistence of rabies at low densities in the Arctic. Chapter 3 uses a temperature-driven moving habitat model for competing host species with a multi-host susceptible-infected disease dynamic for a directly transmitted pathogen. Chapter 3 allows us to understand disease dynamics when a competitor (red fox) invades a species with endemic disease (arctic fox) given climate-induced range shift. These two models help us understand how rabies is being transmitted in the Arctic, and what it will be like in the future, given climate-induced range shifts. Overall, we find that source-sink disease dynamics in the Arctic allow for persistence of rabies in low density patches, and spatial heterogeneity allows the persistence of rabies at landscape-level densities below previously defined disease thresholds for endemicity. Also, we find that there are several plausible scenarios in which

rabies will migrate southward from arctic foxes to red foxes, as both species' distributions shift northward.

1.1 References

Altizer, S., Ostfeld, R. S., Johnson, P. T., Kutz, S., Harvell, C. D., 2013. Climate change and infectious diseases: from evidence to a predictive framework. science 341, 514-519.

Anderson , R. M.., Helen, C. J., Robert, M. M., Anthony, M. S., 1981. Population dynamics of fox rabies in Europe. Nature 289, 765, doi:10.1038/289765a0.

Angerbjörn, A., Tannerfeldt, M., Erlinge, S., 1999. Predator-prey relationships: Arctic foxes and lemmings. J Anim Ecol 68, doi:10.1046/j.1365-2656.1999.00258.x.

Ballard, W. B., Follmann, E. H., Ritter, D. G., Robards, M. D., Cronin, M. A., 2001. Rabies and canine distemper in an artic fox population in Alaska. J Wildl Dis 37, doi:10.7589/0090-3558-37.1.133.

Bellard, C., Thuiller, W., Leroy, B., Genovesi, P., Bakkenes, M., Courchamp, F., 2013. Will climate change promote future invasions? Global Change Biology 19, 3740-3748.

Berestycki, H., Diekmann, O., Nagelkerke, C. J., Zegeling, P. A., 2009. Can a species keep pace with a shifting climate? Bulletin of mathematical biology 71, 399.

Bolker, B., Grenfell, B., 1995. Space, Persistence and Dynamics of Measles Epidemics. Philosophical Transactions: Biological Sciences 348, 309-320.

Brownstein, J. S., Holford, T. R., Fish, D., 2005. Effect of climate change on lyme disease risk in N. America. EcoHealth 2, 38-46, doi:10.1007/s10393-0040139-x.

Chen, I. C., Hill, J. K., Ohlemüller, R., Roy, D. B., Thomas, C. D., 2011. Rapid range shifts of species associated with high levels of climate warming. Science 333, 1024, doi:10.1126/science.1206432.

de Souza, A., Madhusudana, S. N., 2014. Survival from rabies encephalitis. Journal of the Neurological Sciences 339, 8-14, doi:https://doi.org/10.1016/j.jns.2014.02.013.

East, M., Hofer, H., Cox, J., Wulle, U., 2001. Regular exposure to rabies virus and lack of symptomatic disease in Serengeti spotted hyenas. Proceedings of the National Academy of Sciences of the United States of America, 15026-15031.

Gurarie, D., Seto, E. Y., 2008. Connectivity sustains disease transmission in environments with low potential for endemicity: modelling schistosomiasis with hydrologic and social connectivities. Journal of the Royal Society Interface 6, 495-508.

Hagenaars, T. J., Donnelly, C. A., Ferguson, N. M., 2004. Spatial heterogeneity and the persistence of infectious diseases. Journal of Theoretical Biology 229, 349-359, doi:https://doi.org/10.1016/j.jtbi.2004.04.002.

Hales, S., de Wet, N., Maindonald, J., Woodward, A., 2002. Potential effect of population and climate changes on global distribution of dengue fever: an empirical model. The Lancet 360, 830-834, doi:https://doi.org/10.1016/S0140-6736(02)09964-6.

Harris, S., 1981. An estimation of the number of foxes (Vulpes vulpes) in the city of Bristol, and some possible factors affecting their distribution. Journal of Applied Ecology 18, 455-465, doi:10.2307/2402406.

Hersteinsson, P., MacDonald, D. W., 1992. Interspecific competition and the geographical distribution of red and arctic foxes Vulpes vulpes and Vulpes lagopus. Oikos 64, 505-515, doi:10.2307/3545168.

Hethcote, H. W., 1976. Qualitative analyses of communicable disease models. Mathematical Biosciences 28, 335-356.

Hurford, A., Cobbold, C. A., Molnár, P. K., 2019. Skewed temperature dependence affects range and abundance in a warming world. 286. Proc. R. Soc. B.

Martens, W. J., Niessen, L. W., Rotmans, J., Jetten, T. H., McMichael, A. J., 1995. Potential impact of global climate change on malaria risk. Environmental health perspectives 103, 458-464, doi:10.1289/ehp.95103458.

Molnár, P. K., Derocher, A. E., Thiemann, G. W., Lewis, M. A., 2010. Predicting survival, reproduction and abundance of polar bears under climate change. Biological Conservation 143, 1612-1622, doi:https://doi.org/10.1016/j.biocon.2010.04.004.

Molnár, P. K., Kutz, S. J., Hoar, B. M., Dobson, A. P., 2013. Metabolic approaches to understanding climate change impacts on seasonal host-macroparasite dynamics. Ecology Letters 16, 9-21.

Mørk, T., Bohlin, J., Fuglei, E., Åsbakk, K., Tryland, M., 2011. Rabies in the Arctic fox population, Svalbard, Norway. Journal of Wildlife Diseases 47, 945-957, doi:10.7589/0090-3558-47.4.945.

Paradis, A., Elkinton, J., Hayhoe, K., Buonaccorsi, J., 2008. Role of winter temperature and climate change on the survival and future range expansion of the hemlock

woolly adelgid (Adelges tsugae) in eastern North America. Mitigation and adaptation strategies for global change 13, 541-554, doi:10.1007/s11027-007 9127-0.

Patz, J. A., Epstein, P. R., Burke, T. A., Balbus, J. M., 1996. Global climate change and emerging infectious diseases. JAMA 275, 217-223, doi:10.1001/jama.1996.03530270057032.

Peterson, A. T., 2006. Ecologic niche modeling and spatial patterns of disease transmission. Emerging infectious diseases 12, 1822.

Potapov, A. B., Lewis, M. A., 2004. Climate and competition: the effect of moving range boundaries on habitat invasibility. Bulletin of mathematical biology 66, 975-1008.

Pounds, J. A., 2001. Climate and amphibian declines. Nature 410, 639, doi:10.1038/35070683.

Purse, B. V., Mellor, P. S., Rogers, D. J., Samuel, A. R., Mertens, P. P. C., Baylis, M., 2005. Climate change and the recent emergence of bluetongue in Europe. Nature reviews. Microbiology 3, 171-181.

Savory, G. A., Hunter, C. M., Wooller, M. J., O'Brien, D. M., 2014. Anthropogenic food use and diet overlap between red foxes (Vulpes vulpes) and arctic foxes (Vulpes lagopus) in Prudhoe Bay, Alaska. Canadian Journal of Zoology 92, 657-663, doi:10.1139/cjz-2013-0283.

Schwartz, I., 1992. Small amplitude, long period outbreaks in seasonally driven epidemics. Journal of Mathematical Biology 30, 473-491, doi:10.1007/BF00160532.

Stephanson, C., Coe, N., 2017. Impacts of Beech Bark Disease and Climate Change on American Beech. Forests 8, 155, doi:10.3390/f8050155.

Trewhella, W. J., Harris, S., McAllister, F. E., 1988. Dispersal distance, home-range size and population density in the red fox (Vulpes vulpes): A Quantitative Analysis. Journal of Applied Ecology 25, 423-434, doi:10.2307/2403834.

Urban, M. C., Zarnetske, P. L., Skelly, D. K., 2013. Moving forward: dispersal and species interactions determine biotic responses to climate change. Annals of the New York Academy of Sciences 1297, 44-60.

Wasik, B., Murphy, M., 2013. Rabid: A Cultural History of the World's Most Diabolical Virus. Penguin Press.

Wang, W., Zhao, X.-Q., 2004. An epidemic model in a patchy environment. Mathematical Biosciences 190, 97-112, doi:https://doi.org/10.1016/j.mbs.2002.11.001.

Wilfried, T., 2007. Biodiversity: Climate change and the ecologist. Nature 448, 550, doi:10.1038/448550a.

1.2 Co-Authorship Statement

Both manuscripts in this thesis were co-authored with Dr. Amy Hurford, Dr. Nicolas Lecomte, and Dr. Patrick Leighton. I am the principal author for all chapters, and was the principal contributor to project design, model derivation, model analysis, and manuscript preparation.

Chapter 2: Understanding rabies persistence in low-density fox populations

2.1 Abstract

Arctic fox (*Vulpes lagopus*) and its tundra habitat are a unique system for the study of rabies virus epidemics. Contrary to theoretical calculations that report a critical density (K_T) of approximately 1 fox/km^2 for rabies endemicity, arctic rabies persists at densities well below this. The calculation of K_T = 1 fox/km^2 assumes a uniform fox density across the landscape and unrestricted mixing between susceptible and infected foxes. We hypothesize that spatial heterogeneity arising from resource distribution or social structure may result in regions where rabies is endemic, even though average fox densities at the regional or landscape-level are below K_T. To expand upon the limited body of research surrounding the persistence of arctic rabies, we examine arctic rabies via a two-patch structure. We find that rabies can persist in a heterogeneous landscape where the mean carrying capacity is below the threshold carrying capacity required for endemicity in a homogeneous landscape. Rabies endemicity in low-carrying capacity regions within heterogeneous landscapes is further facilitated by high transmission rates, potentially due to 'floater' foxes, and when between-patch movement is restricted to only latently-infected and infected foxes. Our results suggest that rabies may persist in heterogeneous landscapes when the mean carrying capacity is as low as 0.25 foxes per km^2.

2.2 Introduction

Thresholds for disease persistence derived from models assuming homogeneous mixing, and without spatial structure, identify critical densities necessary for disease spread (Keeling and Rohani 2007, Lloyd-Smith et al. 2005). However, those commonly used models can predict densities not found in the field. For instance, Anderson et al. (1981) predicts rabies persistence in Europe when densities of its regional host, red foxes (*Vulpes vulpes*), are as low as 1 fox/km^2, yet rabies persists in the tundra when densities of arctic fox (*Vulpes lagopus*) are well below this threshold (Simon et al. 2019). One way such a contradiction could exist is that environmental heterogeneity may lower threshold host densities for disease persistence. In this scenario, connectivity between populations can facilitate "rescue effects", preventing disease extirpation that would otherwise occur in an equivalent homogenous environment (Hess 1996, Hagenaars et al. 2004). Here, we hypothesize that spatial structure reduces the threshold fox density for rabies persistence, to be consistent with reported arctic fox densities and observed rabies endemicity.

Previous results from metapopulation theory offer additional insights into how spatial structure will affect predicted rabies dynamics. For disease persistence in a metapopulation, at least one of the subpopulations must be able to support the disease independently (Hethcote 1976). For a two-patch model, where only one patch can support the disease independently, either the disease dies out, or persists in both patches, depending on the between-patch connectivity (Wang and Zhao 2004). More generally, pairing two populations with different qualitative or quantitative behavior can lead to the emergence of

new population dynamics and novel spatial patterns (Pedersen et al. 2017). Spatial structure and population connectivity affect persistence and threshold values (Bolker and Grenfell 1995, Wang and Zhao 2004, Wang and Mulone 2003), and once a disease becomes endemic, the intensity of outbreaks and fade-out dynamics can be influenced by the spatial arrangement (Post 1982, Sattenspiel 1987). Considering arctic rabies within a metapopulation structure complements previous research that applies metapopulation theory to communicable diseases such as hepatitis A, gonorrhea, and HIV, which are all characterized by non-homogenous mixing and infections (Lajmanovich and Yorke 1976, Jacquez et al. 1988, Sattenspiel 1987). In these instances, the inclusion of spatial heterogeneity is justified in that humans, as a host, violate homogenous mixing assumptions, since most people use the same travel routes, work in the same areas, and reside in the same locations daily.

Of the various host species and their habitable environments, the arctic fox (*Vulpes lagopus*) and its tundra habitat has proved to be a unique system for the rabies virus. Contrary to the well-documented disease density threshold (K_T) of approximately 1 fox/km^2 (Anderson et al. 1981), arctic rabies persists endemically at densities below this. Indeed, landscape-level arctic fox densities rarely exceed 0.3 breeders/km^2 (Angerbjörn et al. 1999, Eide et al. 2004, Simon et al. 2019). When these numbers are scaled into total number of foxes per square kilometer, by including non-breeding foxes and juvenile survival, Arctic densities are still unlikely to exceed an average of 1 fox/km^2. While most Arctic regions have average densities below K_T, some local areas have carrying capacities that exceed the K_T threshold. These areas are, for instance, town dump sites, migratory bird

colonies, and carrion along caribou migratory pathways, all of which are potentially regions within a metapopulation that can independently support rabies (Harris 1981, Savory et al. 2014, Trewhella et al. 1988), thus meeting Hethcote's (1976) requirement for disease persistence in a metapopulation. In addition, "floater" foxes move between social groups, having high mobility rates, and are an overlooked aspect of arctic rabies persistence.

Previous rabies modeling research provides meaningful insights and shows some agreement with empirical observations. Specifically, previous models predict spread rates (Källén et al. 1985, Murray et al. 1986, Smith et al. 2002), and define thresholds for vaccination regimes and efficient implementation (Asano et al. 2008, Broadfoot et al. 2001, Clayton et al. 2010, Neilen et al. 2011, Russell et al. 2006). When the carrying capacity of all foxes in an area is greater than the threshold density ($K>K_T$), either dampened oscillations or limit cycles result, and these characteristics have been well documented in the epidemiological data of red fox populations across Europe and most of North America (Anderson et al. 1981). Still, many critical questions, such as the spread and maintenance of rabies in the Arctic, are largely unresolved (Mork and Prestrud 2004). Simon et al. (2019), extends Anderson et al. (1981) to consider high transmission rates, short incubation periods, prolonged infectious periods, periodicity in the birth rate, and interaction with red foxes. With these modifications to Anderson's model, rabies can persist in the Arctic with fox densities lower than 0.15 fox/km^2, yet at low densities, immigration will cause sporadic outbreaks of rabies, and this leaves open the question of dispersal's role in rabies endemicity (Simon et al. 2019).

Without spatially structured source-sink disease dynamics, host interactions are not partitioned into a biologically representative scheme, but are represented as an average; without spatial structure the potential for rescue effects and disease reintroduction is eliminated. Here, we formulate and parameterize a two-patch disease model to explore rabies persistence in the Arctic and disease dynamics in low-density regions. We identify the necessary conditions for rabies endemicity in a metapopulation and consider how rabies can persist at landscape-level densities below K_T, given the assumptions our model makes about space, connectivity, and individuals.

2.3 Methods

Two-patch model

We use a two-patch deterministic model (Figure 2.1). One of the two patches is a low-carrying capacity patch ($K_1<K_T$) that is characteristic of many Arctic areas (hereafter referred to as the 'sink patch', and where tundra specific variables and parameters are indexed with a subscript 1). The sink patch is coupled with a higher-carrying capacity patch ($K_2 > K_1$) to represent the area surrounding a town, migratory pathway, or a migratory bird colony (hereafter referred to as the 'source patch', where specific variables and parameters are indexed with a subscript 2).

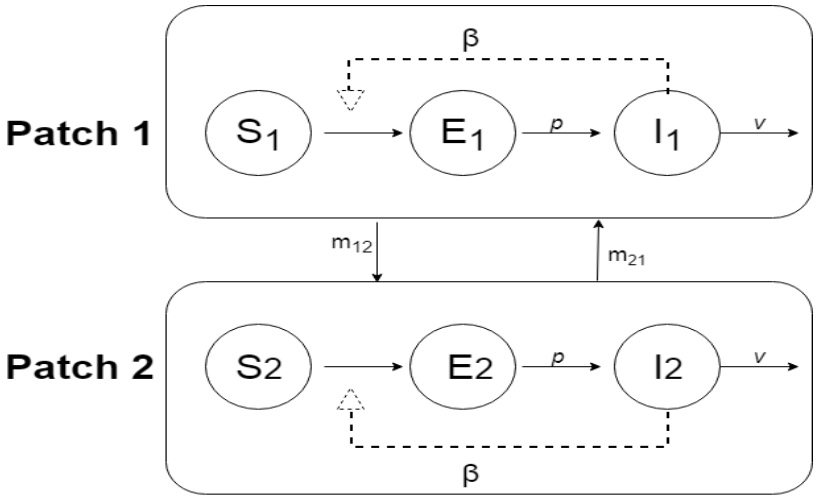

Figure 2.1: A two-patch model describing rabies dynamics. The epidemiological status of foxes are susceptible, S_1 and S_2; latent, E_1 and E_2; and infected, I_1 and I_2, where the subscript 1 indicates residence on a sink (low-carrying capacity) patch and the subscript 2 indicates residence on a source patch (high-carrying capacity). The transmission rate is β, the rate of disease progression from exposed to infected is *p*, and the disease-induced mortality rate is *v*. The inter-patch movement rate, from a patch *i* to *j* is m_{ij} and the epidemiological status of foxes does not change while travelling between patches. The model assumes that each of these parameters (β, *p*, and *v*) are the same for all individuals. The figure does not show reproduction, mortality, or density dependent constraints for visual clarity. See equations 1-6 for the complete model.

The within-patch epidemiological dynamics, including density-dependent population growth, are based on Anderson et al. (1981). Within a patch, *i*, the model variables describe the density of susceptible, S_i, latent or exposed, E_i, and infected, I_i, foxes (fox/km^2), and the model does not consider recovery as rabies is almost always fatal. The density on patch *i* is $N_i = S_i + E_i + I_i$, and rabies percent prevalence is defined as $((E_i + I_i)/N_i) \cdot 100$, which is a percent ranging between 0 and 100. The rate that each susceptible fox is exposed to rabies per infected fox is β (foxes/km^2)$^{-1}$ yr^{-1} (transmission dynamics assume mass action). The rate of disease progression from E_i to I_i is *p*, and the rate of disease-induced mortality for infected individuals is *v* (both with units yr^{-1}). Our formulation assumes that only foxes susceptible to rabies (S_1 and S_2) can reproduce, as the degenerative effects of rabies make it unlikely that foxes of any other epidemiological status would be able to reproduce, and assumes that pups are born susceptible. Foxes disperse between patches at the rate m_{ji} from patch j to i. Parameter values are the same on both patches except interpatch dispersal, m_{ji}, and the carrying capacity, K_i, which appears in equations 1-6 via μ_i, since $\mu_i = r/K_i$ (i.e. see Table 1). The model dynamics are,

$$\dot{S}_1 = rS_1 - \mu_1 S_1 N_1 - \beta S_1 I_1 - S_1 m_{12} + S_2 m_{21}, \quad (1)$$

$$\dot{E}_1 = \beta S_1 I_1 - E_1(p + d) - \mu_1 E_1 N_1 - E_1 m_{12} + E_2 m_{21}, \quad (2)$$

$$\dot{I}_1 = pE_1 - I_1(v + d) - \mu_1 I_1 N_1 - I_1 m_{12} + I_2 m_{21}, \quad (3)$$

$$\dot{S}_2 = rS_2 - \mu_2 S_2 N_2 - \beta S_2 I_2 - S_2 m_{21} + S_2 m_{12}, \quad (4)$$

$$\dot{E}_2 = \beta S_2 I_2 - E_2(p + d) - \mu_2 E_2 N_2 - E_2 m_{21} + E_2 m_{12}, \quad (5)$$

$$\dot{I}_2 = pE_2 - I_2(v+d) - \mu_2 I_2 N_2 - I_2 m_{21} + I_2 m_{12}. \quad (6)$$

Table 2.1: Parameter descriptions for the two-patch rabies model (equations 1-6). Parameters are the same as Anderson et al. (1981) and Simon et al. (2019), but where subscripts denote patch specific values. The parameter values are the same on each patch, except for carrying capacity and dispersal.

definition	***parameter***	***value***
Birth rate	a	1 yr^{-1}
Mortality	d	0.5 yr^{-1}
Net population growth rate at low densities	$r=a-d$	0.5 yr^{-1}
Patch 1 dispersal	m_{12}	0.1 - 0.25 yr^{-1}
Patch 2 dispersal	m_{21}	0.1 – 80 yr^{-1}
Patch 1 carrying capacity	K_1	0.0 – 1.0 fox/km^2
Patch 2 carrying capacity	K_2	0.1 – 5.0 fox/km^2
Latency	p	13 yr^{-1}
Disease-induced mortality	v	73 yr^{-1}
Transmission coefficient	β	80 km^2/fox·yr
Density-dependent constraints	$\mu_i=r/K_i$	Varied km^2/fox·yr

Parameter values provided in Table 1 are based on Anderson et al. (1981) and Simon et al. (2019) to provide comparable results to equivalent spatially homogenous models. The parameter values were also cross-referenced with Mork and Prestrud (2004) to ensure they were biologically relevant for arctic fox populations.

To estimate carrying capacity, we assumed that the estimated densities of foxes are near carrying capacity and we included breeding pairs, juveniles that remain at the den, and adult non-breeding foxes (floaters). The density of breeders is estimated as 0.02-0.3 breeders/km^2 (Angerbjörn et al. 1999). The regression given by Strand et al. (1995) estimates litter size from placental scars, giving an average litter of 9 pups for a breeding pair. Pup to juvenile survival is about 10% (Miejer et al. 2008), so there are approximately

0.45 juvenile foxes/breeder/year. Next, we consider floaters, which have been documented as up to 25% of the population (Lindstrom 1989), and for this study we assume floaters are on average 20% of the population. The carrying capacity estimate, per breeder, is $(1+0.45)/0.8 = 1.81$. As the density of breeding pairs spans a range that is 15x greater than its lower bound, we will estimate low-, mid- and high- carrying capacity values for the sink patch to acknowledge this uncertainty. Our estimates for the carrying capacity on the sink patch are:

$$K_1 = 0.02 \cdot 1.81 = 0.036 \text{ fox}/ km^2 \text{ (Low)},$$

$$K_1 = 0.16 \cdot 1.81 = 0.29 \text{ fox}/ km^2 \text{ (Mid)},$$

$$K_1 = 0.3 \cdot 1.81 = 0.54 \text{ fox}/ km^2 \text{ (High)}.$$

The transmission rate for rabies is estimated to be $\beta = 80\ km^2/\text{fox} \cdot \text{yr}$ (Anderson et al. 1981, Llyod 1980). However, it is unclear whether this estimate is calculated for resident foxes or also considers highly mobile 'floaters', which may be 7-10 times more mobile (Lindstrom 1989). When floaters are excluded from the β estimate, and given our previous assumption that floaters are 20% of the population, an estimate of the transmission rate that considers floaters would range from $\beta = 176\ to\ 224\ km^2/\text{fox} \cdot \text{yr}$.

To perform our analyses, we numerically solved equations (1-6) using the ode45 function in MATLAB 2018a until the total population size reached an equilibrium state. The system of equations and the computer code are available via the following link: https://doi.org/10.6084/m9.figshare.c.4840710

2.4 Results

Low to intermediate levels of dispersal in heterogeneous environments can support rabies in low-carrying capacity 'sink' patches, where rabies would be absent if the patch were isolated, or if the landscape was homogeneous with the carrying capacity equal to this low value, K_1 (Figure 2.2). As the carrying capacity on the sink patch increases toward the threshold carrying capacity in a homogeneous environment, K_T, the sink patch requires less augmentation via dispersal from the source patch to maintain disease, which is reflected by the expanding parameter space for endemicity as shown for the low- (Figure 2.2a), mid- (Figure 2.2b), and high- (Figure 2.2c) estimates for K_1. Disease is supported in the sink patch until dispersal from the source patch removes too many susceptible and infected foxes, such that disease dynamics cannot be maintained on the source patch, at which point, the disease dies out in both patches (Figure 2.2).

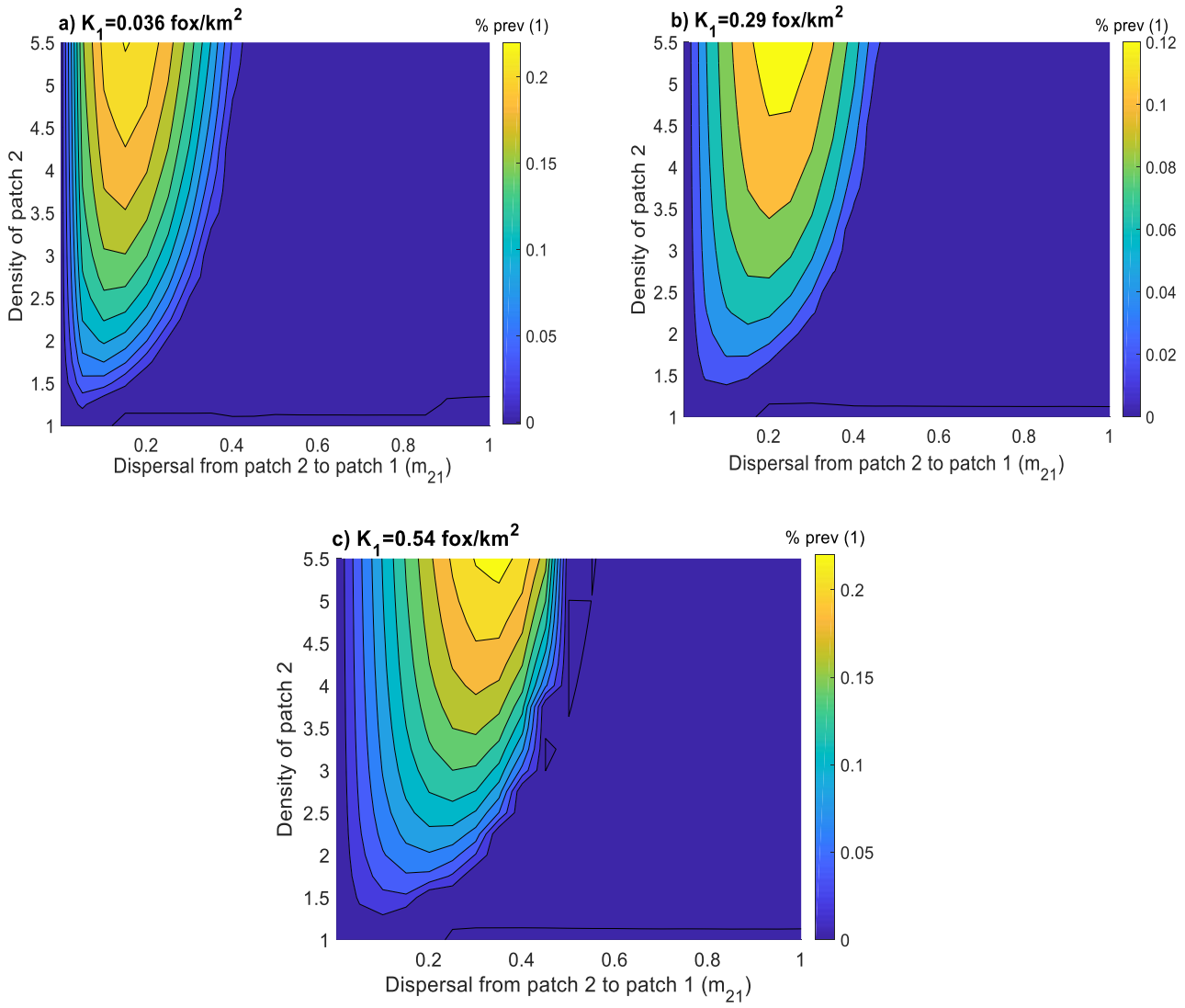

Figure 2.2: Rabies is endemic to the sink patch (low-carrying capacity), where disease would otherwise be absent, when low to intermediate levels of movement couples the disease dynamics between the sink and source (high-carrying capacity) patches. Panels show rabies prevalence, $(100(E_1+I_1)/N_1)$, on the sink patch for our three estimates of carrying capacity with K_1 equal to low: 0.036 (a); mid: 0.29 (b), and high: 0.54 (c) fox/km^2. Rabies prevalence (%) on the sink patch is highest for large values of the carrying capacity in the source (large K_2), large values of the carrying capacity in the source (c; high estimate of K_1), and for intermediate movement rates to the sink from the source patch (m_{21}), a pattern that is explained further in Figure 2.3. Parameters value are given in Table 2.1 and m_{12}=0.25.

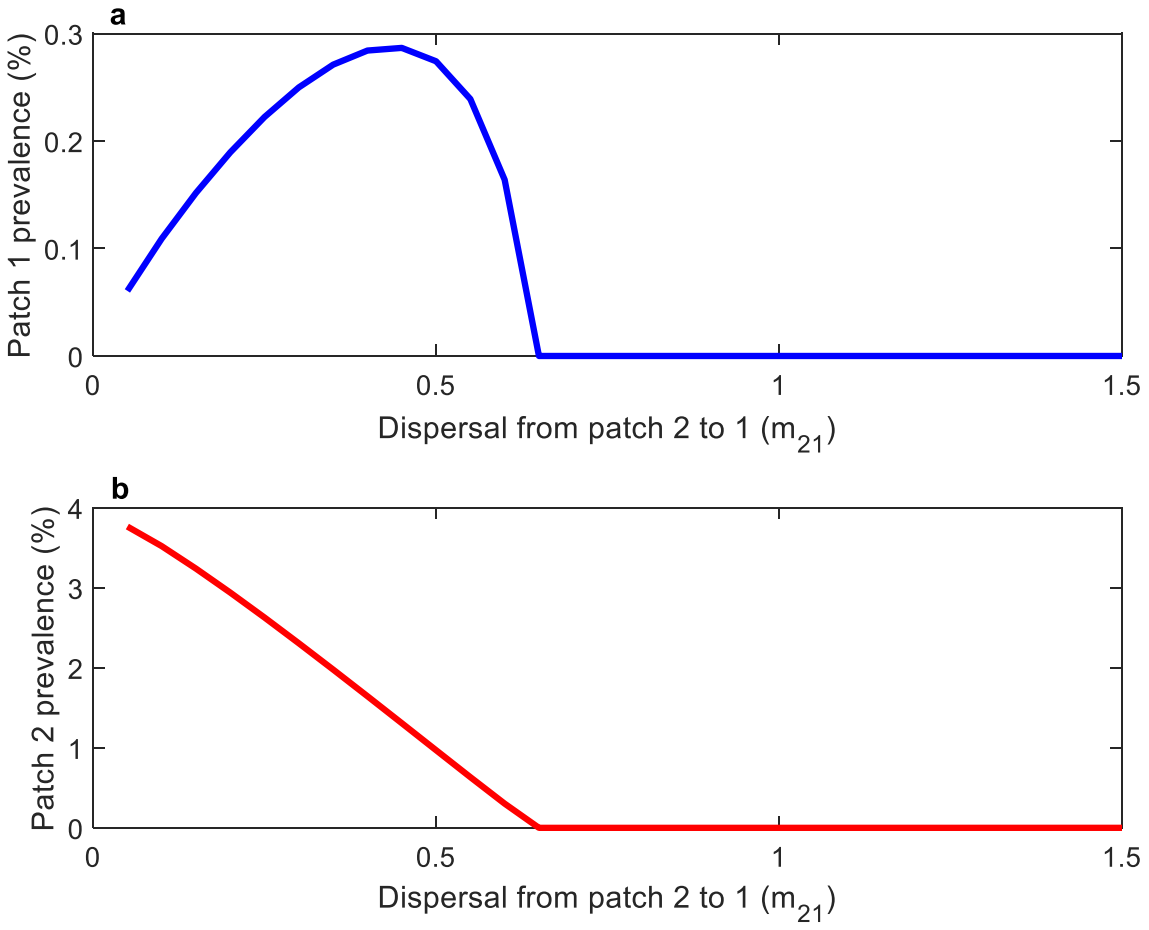

Figure 2.3: Rabies prevalence (%) on the sink patch (a) peaks at intermediate movement rates because high movement rates eradicate the infection in the source patch (b). For high levels of movement, the source patch cannot maintain its function as a disease source when the density of susceptible and infected foxes are depleted through movement and become too few to sustain the epidemic. Parameters values are given in Table 2.1, with $m_{12} = 0.25$, $K_1 = 0.54$ fox/km^2, and $K_2 = 5$ fox/km^2.

In a heterogeneous two-patch landscape, rabies can persist when the landscape-level mean carrying capacity is below the threshold carrying capacity for rabies endemicity in a homogeneous landscape, K_T (Figure 2.4). When the landscape-level mean carrying capacity is fixed at 0.9 foxes/km^2, and different combinations of K_1 and K_2 are considered, we find that rabies prevalence is highest when the carrying capacities on

the sink and source patches are the most different (Figure 2.4). However, for lower values of the landscape-level mean carrying capacity, for example $\overline{K}$=.5 fox/km^2, rabies endemicity is not possible (see appendix figure A.1), as infection prevalence on the source patch is too low to both sufficiently subsidize the sink patch and maintain disease locally.

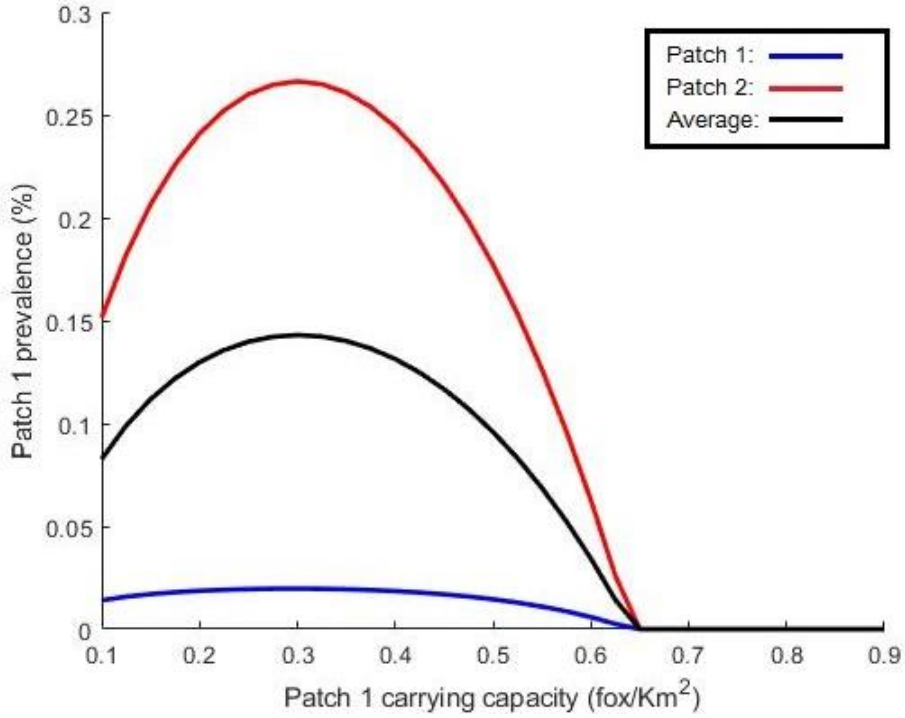

Figure 2.4: Rabies can be endemic in a heterogeneous landscape where the mean carry capacity is less than the threshold carrying capacity for rabies endemicity in a homogeneous landscape. For our parameter values (Table 1), rabies is endemic in a homogenous landscape when the carrying capacity is greater than 1 fox/km^2 ($K>K_T=1$; (Andersen and May (1981)). We set the landscape-level mean carrying capacity for our two-patch model to $\overline{K} = (K_1 + K_2)/2 = 0.9$ foxes/km^2**.** When $K_1=K_2=\overline{K} =0.9< K_T$ (far right on the x-axis), no disease occurs on either patch since the landscape is homogeneous, however, as the variance between the two carrying capacities on each patch increases (toward the left on the x-axis) rabies becomes established on both patches (red and blue lines). The between-patch movement rates are $m_{12}=m_{21}=0.25$, and all other parameter values are as given in Table 2.1.

We estimate that rabies can persist for fox populations in heterogeneous environments where the mean carrying capacity is as low as ~0.25 foxes/km^2 and the carrying capacity in the sink patch is as low as 0.036 foxes/km^2 (Figure 2.5). To generate this lower bound, we considered the maximum feasible estimate of β= 224 km^2/fox·yr and our lowest estimate of fox carrying capacity.

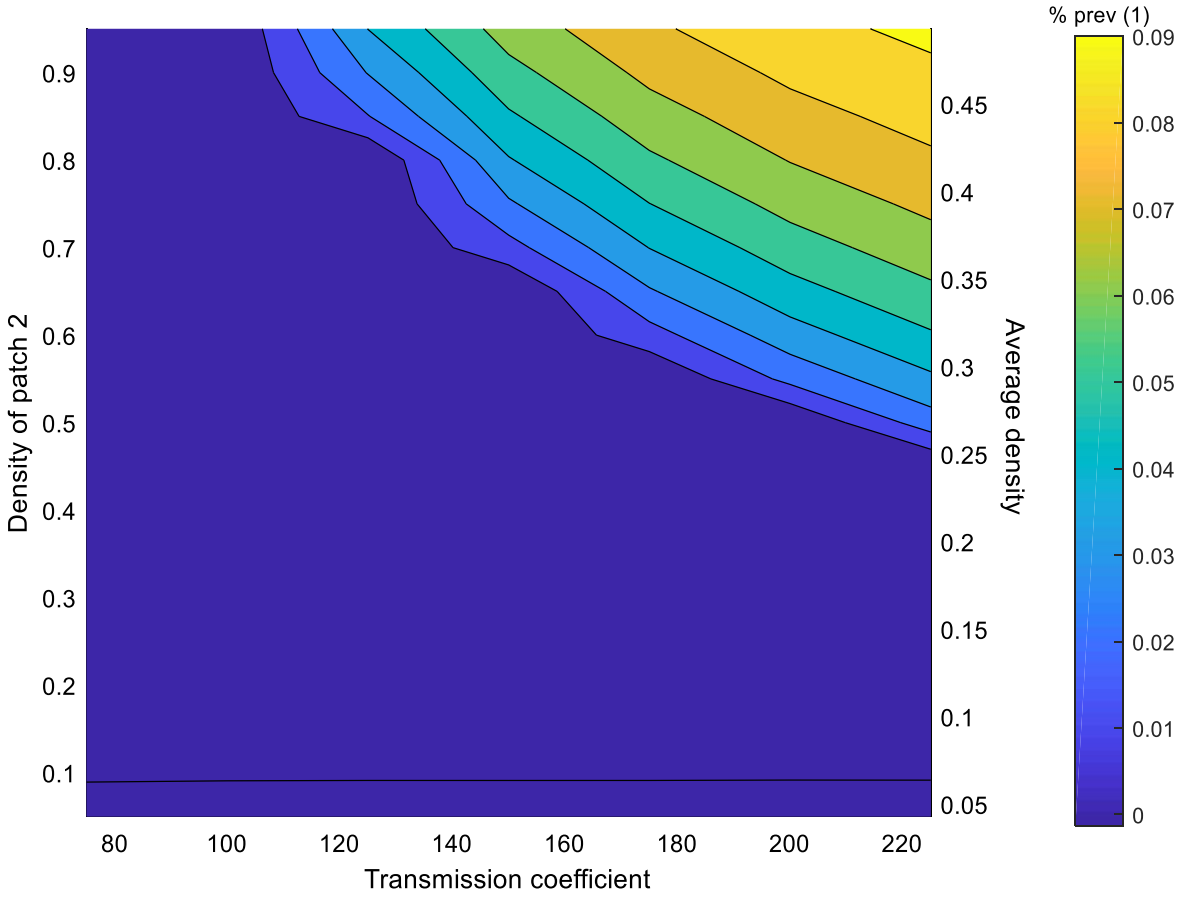

Figure 2.5: Higher transmission rates, for example, due to highly mobile 'floater' foxes, allow for rabies endemicity for landscape-level carrying capacities as low as 0.25 foxes/km^2. The transmission rate is elevated by floaters or higher mobility foxes (we consider a range of values beginning from the baseline value of 80 and increase to 224 km^2 foxes^{-1} yr^{-1}). With the carrying capacity on the sink patch set to its lowest estimate: K_1=.036 fox/km^2, we find that rabies can persist when the carrying capacity on the source patch is ~0.46 foxes/km^2 (the value of K_2 for the blue contour when β= 224 km^2/foxes^{-1} yr^{-1}) corresponding to a landscape-level mean carrying capacity of ~0.25 foxes/km^2, as seen on the right y-axis. Parameter values are m_{12}=m_{21}=0.1 yr^{-1}, and all other parameters are as described in Table 2.1.

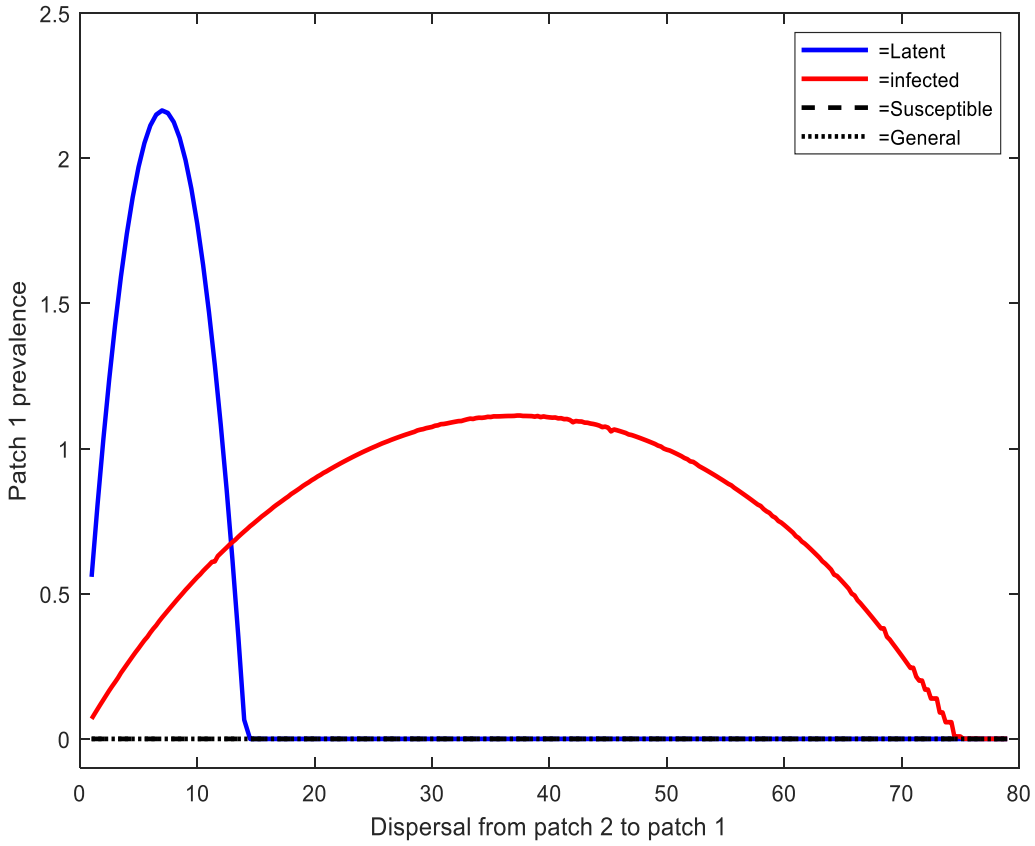

Figure 2.6: Rabies can be endemic on the sink patch, when it might otherwise be eliminated (black), if between-patch movement occurs for only infected foxes (red) or only latent foxes (blue). Assuming that between-patch movement occurs for foxes with all epidemiological statuses or only for susceptible foxes, then rabies is cannot persist for a wide range of movement rates from the source to the sink patch (black dashed and dotted lines), but when assuming only infected foxes move between patches rabies is present on the sink patch for a wide range of movement rates (red). Assuming that only latent foxes move between patches, rabies prevalence on the sink patch can be high, but results in the extinction of the fox population for high movement rates (blue). The model formulation is described in Appendix A.1 and parameters are given in Table 2.1, with $K_2 = 2$ fox/km^2, $K_1 = 0.54$ fox/km^2, and $m_{12} = 0.25$ yr^{-1}.

We found that rabies persistence is sensitive to our assumptions restricting the epidemiological status of dispersing foxes (Figure 2.6). We set $K_1 = 0.54$ foxes/km^2 and $K_2 = 2$ foxes/km^2 and found that irrespective of the level of dispersal from the source to the sink patch, rabies could never persist if all epidemiological compartments disperse equally, or if only susceptible foxes disperse, for a dispersal rate >1 yr^{-1} (Figure 2.6, black lines). By contrast, rabies did persist when only latent or infected foxes disperse (Figure 2.6, blue and red lines). Rabies persistence occurred over the widest range of ecological conditions when only infected foxes dispersed, however, rabies prevalence reached its highest value when only latent foxes disperse.

2.5 Discussion

Low fox densities and spatial discontinuity heavily influence rabies disease dynamics in the Arctic. Spatially homogenous disease models, which assume uniform density and mixing, typically give a useful simplification of infection dynamics, as seen in Anderson et al. (1981). The increased resolution that heterogeneity gives a model is especially important near threshold values, where small changes can shift the qualitative outcome of a deterministic model. Using spatial heterogeneity as a lens to view arctic rabies, we extended the work of Simon et al. (2019) whereby infected animals subsidize the system via an unspecified source without any dynamics. Doing so, we determined the conditions in which rabies can persist in the Arctic under a two-patch structure, where infectious individuals move between source and sink patches.

We showed endemicity in the low-carrying capacity patch when paired with a higher carrying capacity disease source patch. This was observed across a range of low-densities and dispersal values (Figure 2.2), and when latent only or infected only individuals move between patches (Figure 2.6). We found that rabies can persist when the average carrying capacity, $\overline{K} = (K_1+K_2)/2$, across the two patches in the metapopulation is less than $K_T = 1$ fox/km^2 (Figure 2.4). Our results are consistent with previous studies. Like Hethcote (1976), we found that for a low-carrying capacity patch to support disease, the subsidization from the source patch must not be so much that it suppresses disease dynamics in that patch (Figure 2.3). We also found equilibrium rabies prevalence in the metapopulation peaks with low—level symmetric bi-directional dispersal (Figure 2.2) as noted in Gurarie et al. (2008), and further extend those results by showing that high levels

of dispersal can maximize disease prevalence when only latently-infected, or infectious individuals disperse (Figure 2.6).

We examined the potential for higher mobility of arctic foxes via the transmission coefficient, β, as floater foxes may play a major role in disease transmission. We showed endemicity in all low-carrying capacity patches across a wide range of β values, and for larger β values, even when the source patch carrying capacity (K_2) was well below K_T (Figure 2.5). Figures 2.2 and 2.4 shows the plausibility of rabies on low carrying capacity patches, however, if we assume that the neurological effects of rabies makes its host the most likely demographic to disperse (Figure 2.6), then there is a much larger parameter space that will allow for rabies persistence in the Arctic than seen in Figure 2.2. This is particularly relevant, given that specific strains of the virus can influence the dispersal and habitat permeability to infected individuals (Scott 1988), and rabies alters dispersal and movement patterns (Barton et al. 2010), which is in contrast to the well-studied territoriality and demographic dispersal events observed in fox populations.

We independently considered several mechanisms that facilitated rabies endemicity at low carrying capacity, yet it is likely that many of these mechanisms are working in combination to create an environment where rabies is endemic at extremely low densities. Furthermore, we used a two-patch system, however, additional patches would allow for a lower threshold for endemicity, as a single patch could potentially experience the additive effects of multiple patches contributing to or subsidizing that single patches population and disease dynamics. With the presence of a disease reservoir, i.e., around towns or goose colonies, floater foxes with higher transmission rates, and dispersal of foxes with latent or

clinical rabies infection, we suggest it is feasible to have rabies endemicity in landscapes where the average landscape density is 0.25 fox/km^2, and where sink patches have fox densities of 0.036 fox/km^2 (see Figure 2.5 for details). Whereas we consider patch dynamics in the context of spatial heterogeneity and the related assumptions, it has also been noted that positive temporal autocorrelation and dispersal can enhance metapopulation persistence (Matthews and Gonzalez 2007), even when that metapopulation is composed entirely of sinks (Manojit et al. 2005).

A discrete-patch metapopulation ensemble resembles the structure of the Arctic: the discrete patches are disconnected by several land masses (e.g. mainland Canada), island systems (e.g. Greenland), and archipelagos (e.g. Svalbard) connected by sea ice. Genetic studies show that strains of rabies are spread between these patches, as consistent with the assumptions of metapopulation epidemic models for arctic foxes (Hanke et al. 2016, Raundrup et al. 2015). The geography of Svalbard, an endemically infected area, is consistent with the discrete space assumption of a disease metapopulation model. The most likely origin of rabies in Svalbard is via the migration of arctic foxes from Greenland or the Siberian islands (Mork et al. 2011). On the Spitzenbergen island in Svalbard, the density of breeding foxes is approximately 0.1-0.15 fox/km^2 with prevalence values of ~0.3% (Eide 2002, Mansfield et al. 2006, Mork et al. 2011). These results closely mirror those seen in our low-carrying capacity patches when connected to a disease source.

Rabies is usually absent on the island of Newfoundland, but in the spring of 2002, Newfoundland saw its first outbreak of rabies in 14 years (Nadin-Davis et al. 2008). It is assumed that the disease was introduced to the island from an infected mainland fox that

travelled on an ice sheet across the 9-mile strait from Labrador. This outbreak captures the essence of arctic rabies; it is a disease that is largely governed by the spatial arrangement of the Arctic and its connectivity. Here, we examined arctic rabies through this lens using a two-patch structure, and found that rabies can persist endemically in the Arctic via source-sink dynamics, partitioning of densities, selective dispersal, and increased mobility. These all provided realistic parameter space for rabies endemicity, further supported by the disease dynamics observed in Arctic regions characterized by a metapopulation structure. Our study expanded upon the limited body of research surrounding the persistence of arctic rabies, and showed the feasibility of endemicity at low densities by considering spatial dynamics.

2.6 References

Anderson, M. R., Helen, C. J., Robert, M. M., Anthony, M. S., 1981. Population dynamics of fox rabies in Europe. Nature 289, 765.

Angerbjörn, A., Tannerfeldt, M., Erlinge, S., 1999. Predator-prey relationships: Arctic foxes and lemmings. Journal of Animal Ecology 68, 34-49.

Angerbjörn, A., Tannerfeldt, M., Bjärvall, A., Ericson, M., From, J., Noren, E., 1995. Dynamics of the Arctic fox population in Sweden. Annales Zoological Fennici 32, 55-68.

Asano E., Gross L., Lenhart S., Real L.A., 2008. Optimal control of vaccine distribution in a rabies metapopulation model. Mathematical Biosciences and Engineering 5, 219-238.

Barton, H. D., Gregory, A. J., Davis, R., Hanlon, C. A., Wisely, S. M., 2010. Contrasting landscape epidemiology of two sympatric rabies virus strains. Molecular Ecology 19, 2725-2738, doi:10.1111/j.1365-294X.2010.04668.x.

Brauer, F., van den Driessche, P., 2001. Models for transmission of disease with immigration of infectives. Mathematical Biosciences 171, 143-154,

Blackwood J.C., Streicker D.G., Altizer S. & Rohani P., 2013. Resolving the roles of immunity, pathogenesis, and immigration for rabies persistence in vampire bats. Proceedings of the National Academy of Sciences of the United States of America 110, 20837–20842.

Bolker, B., Grenfell, B., 1995. Space, Persistence and dynamics of measles epidemics. Philosophical Transactions: Biological Sciences 348, 309-320.

Broadfoot, J. D., Rosatte, R. C., O'Leary, D. T., 2001. Raccoon and skunk population models for urban disease control planning in Ontario, Canada. Ecological Applications 11, 295-303.

Clayton T., Duke-Sylvester S., Gross L.J., Lenhart S., Real L.A., 2010. Optimal control of a rabies epidemic model with a birth pulse. Journal of Biological Dynamics, 4, 43-58.

Eide, N. E., Jepsen, J. U., Prestrud, P., 2004. Spatial organization of reproductive Arctic foxes *Alopex lagopus*: responses to changes in spatial and temporal availability of prey. Journal of Animal Ecology 73, 1056-1068.

Eide, N.E., 2002. Spatial ecology of arctic foxes. Relations to resource distribution, and spatiotemporal dynamics in prey abundance. Doctor Scientiarum Thesis, Agricultural University of Norway, A˚ s, Norway, 82 pp.

Gurarie, D., Seto, E. Y., 2008. Connectivity sustains disease transmission in environments with low potential for endemicity: modelling schistosomiasis with hydrologic and social connectivities. Journal of the Royal Society Interface 6, 495-508.

Hagenaars, T. J., Donnelly, C. A., Ferguson, N. M., 2004. Spatial heterogeneity and the persistence of infectious diseases. Journal of Theoretical Biology 229, 349-359.

Hanke, D., Freuling, C. M., Fischer, S., Hueffer, K., Hundertmark, K., Nadin-Davis, S., Marston, D., Fooks, A. R., Bøtner, A., Mettenleiter, T. C., Beer, M., Rasmussen, T. B., Müller, T. F., Höper, D., 2016. Spatio-temporal analysis of the genetic

diversity of Arctic rabies viruses and their reservoir hosts in Greenland. PLOS Neglected Tropical Diseases 10.

Harris, S., 1981. An estimation of the number of foxes (*Vulpes vulpes*) in the City of Bristol, and some possible factors affecting their distribution. Journal of Applied Ecology 18, 455-465.

Hethcote, H. W., 1976. Qualitative analyses of communicable disease models. Mathematical Biosciences 28, 335-356.

Hess, G., 1996. Disease in metapopulation models: implications for conservation. Ecology 77, 1617-1632.

Jacquez, J. A., Simon, C. P., Koopman, J., Sattenspiel, L., Perry, T., 1988. Modeling and analyzing HIV transmission: the effect of contact patterns. Mathematical Biosciences 92, 119-199.

Källén A., Arcuri P., Murray J.D., 1985. A simple model for the spatial spread and control of rabies. Journal of Theoretical Biology, 116, pp. 377-393

Keeling, M. R., P, 2008. Modeling Infectious Disease in Humans and Animals. Princeton University Press, Princeton.

Lajmanovich, A., Yorke, J. A., 1976. A deterministic model for gonorrhea in a nonhomogeneous population. Mathematical Biosciences 28, 221-236.

Lindström, E., 1989. Food limitation and social regulation in a red fox population. Ecography 12, 70-79.

Lloyd-Smith, J. O., Cross, P. C., Briggs, C. J., Daugherty, M., Getz, W. M., Latto, J., Sanchez, M. S., Smith, A. B., Swei, A., 2005. Should we expect population thresholds for wildlife disease? Trends in Ecology & Evolution 20, 511-519.

Matthews, D. P., Gonzalez, A., 2007. The inflationary effects of environmental fluctuations ensure the persistence of sink metapopulations. Ecology 88, 2848-2856.

Mansfield, K. L., Racloz, V., McElhinney, L. M., Marston, D. A., Johnson, N., Rønsholt, L., Christensen, L. S., Neuvonen, E., Botvinkin, A. D., Rupprecht, C. E., Fooks, A. R., 2006. Molecular epidemiological study of Arctic rabies virus isolates from Greenland and comparison with isolates from throughout the Arctic and Baltic regions. Virus Research 116, 1-10.

Meijer, T., Norén, K., Hellström, P., Dalén, L., Angerbjörn, A., 2008. Estimating population parameters in a threatened Arctic fox population using molecular tracking and traditional field methods. Animal Conservation 11, 330-338.

Mørk, T., Prestrud, P., 2004. Arctic rabies – A Review. Acta Veterinaria Scandinavica 45, 1.

Mørk, T., Bohlin, J., Fuglei, E., Åsbakk, K., Tryland, M., 2011. Rabies in the Arctic fox population, Svalbard, Norway. Journal of Wildlife Diseases 47, 945-957.

Murray J.D., Stanley E.A., Brown D.L, 1986. On the spatial spread of rabies among foxes. Proceedings of the Royal Society of London Series B. 229, 111–150.

Nadin-Davis, S., Muldoon, F., Whitney, H., Wandeler, A. I., 2008. Origins of the rabies viruses associated with an outbreak in newfoundland during 2002–2003. Journal of Wildlife Diseases 44, 86-98.

Neilan R.M., S. Lenhart, 2011. Optimal vaccine distribution in a spatiotemporal epidemic model with an application to rabies and raccoons. Journal of Mathematical Analysis and Applications, 378, 603-619

Pedersen, E. J., Marleau, J. N., Granados, M., Moeller, H. V., Guichard, F., 2016. Nonhierarchical dispersal promotes stability and resilience in a tritrophic metacommunity. The American Naturalist, 187, E116-E128.

Post, W. M., DeAngelis, D. L., Travis, C. C., 1983. Endemic disease in environments with spatially heterogeneous host populations. Mathematical Biosciences 63, 289 302, doi:https://doi.org/10.1016/0025-5564(82)90044-X.

Raundrup, K., M. Moshøj, C., E. Wennerberg, S., M. O. Kapel, C., 2015. Spatiotemporal distribution of rabies in Arctic foxes in Greenland. European Journal of Wildlife Research 61, 457-456.

Roy, M., Holt, R. D., Barfield, M., 2005. Temporal autocorrelation can enhance the persistence and abundance of metapopulations comprised of coupled sinks. The American Naturalist 166, 246-261.

Russell, C.A., Real, L.A., Smith, D.L., 2006. Spatial Control of Rabies on Heterogeneous Landscapes. PLOS ONE 1, e27.

Sattenspiel, L., 1987. Epidemics in nonrandomly mixing populations: a simulation. American Journal of Physical Anthropology 73, 251-265.

Savory, G. A., Hunter, C. M., Wooller, M. J., O'Brien, D. M., 2014. Anthropogenic food use and diet overlap between Red foxes (*Vulpes vulpes*) and Arctic foxes (*Vulpes lagopus*) in Prudhoe Bay, Alaska. Canadian Journal of Zoology 92, 657-663.

Scott, M. E., 1988. The impact of infection and disease on animal populations: implications for conservation biology. Conservation Biology 2, 40-56, doi:10.1111/j.1523-1739.1988.tb00334.x.

Simon, A. Hurford, A., Lecomte, N. Belanger, D. & P. A. Leighton, 2019. Dynamics and persistence of rabies in the Arctic. Polar Research, 38.

Smith, D. L., Lucey, B., Waller, L. A., Childs, J. E., Real, L. A., 2002. Predicting the spatial dynamics of rabies epidemics on heterogeneous landscapes. Proceedings of the National Academy of Sciences 99, 3668.

Strand, O., Skogland, T., Kvam, T., 1995. Placental scars and estimation of litter size: an experimental test in the Arctic fox. Journal of Mammalogy 76, 1220-1225.

Trewhella, W. J., Harris, S., McAllister, F. E., 1988. Dispersal distance, home-range size and population density in the Red fox (*Vulpes vulpes*): a quantitative analysis. Journal of Applied Ecology 25, 423-43.

Wang, W., Mulone, G., 2003. Threshold of disease transmission in a patch environment. Journal of Mathematical Analysis and Applications 285, 321-335.

Wang, W., Zhao, X.-Q., 2004. An epidemic model in a patchy environment. Mathematical Biosciences 190, 97-112.

World Health Organization, 1990. Report of a WHO/NV1 workshop on Arctic rabies. WHO, 1-21.

Chapter 3: When host populations move north, but disease moves south: counter-intuitive impacts of climate warming on disease dynamics

3.1 Abstract

Climate change is linked to the poleward spread of wildlife ranges and their corresponding diseases. This relationship is supported by countless observations, empirical measurements, and predictions that explore poleward movement in response to a warming climate. We consider an alternative scenario whereby disease moves southward rather than northward in response to climate induced range shifts. This is particularly relevant to viral, bacterial, and prion diseases that do not have thermal tolerance limits and are inextricably linked to their hosts distribution. We formulate a moving habitat integrodifference model with a Susceptible-Infected epidemiological structure for two competing species with different temperature-dependent niche spaces. We present a scenario in which climate change facilitates disease movement southward through space as climate warming moves our niche space northward. There is a tendency to focus on northern latitudes as they generally experience a higher degree of warming relative to southern latitudes; however, our results show that there is a counterintuitive scenario in which southern species may see an increase risk for disease outbreaks and incidence in response to climate change. We explore this in the context of rabies in arctic and red fox. We note the potential for

southward spread and further spillover to additional hosts as the disease moves south, presenting an increasing zoonotic threat.

3.2 Introduction

Many studies observe northward shifts in disease range in the same direction as climate warming induced northward shifting thermal isoclines (Bellard et al. 2013, Patz et al. 1996, Short et al. 2017). In the Northern hemisphere, disease may spread northwards when pathogen fitness closely tracks environmental temperature, either due to host or vector responses to temperature e.g., Lyme disease (Brownstein et al. 2005), or due to pathogen life stages that are exposed to the environment e.g., chytrid fungus (Pounds 2001). However, climate warming also changes host-host contact rates, and may facilitate disease spread into susceptible populations that have previously been isolated, possibly in the south. We hypothesize that climate warming may induce southward disease spread when uninfected, susceptible, southern population individuals disperse northward to where the climate is now warmer, and contact infected individuals in the northern population, thus "connecting" the two populations and facilitating a southward wave of disease.

The spatial isolation necessary for southern disease spread may be a characteristic of multi-host disease systems. In a multi-host system, disease can spread to another host species given sufficient between-species contact rates, however, due to niche partitioning, there are numerous examples of host species that are isolated, with contact rates that are too small for disease to spread between species, e.g., the competitive exclusion of red squirrels by introduced grey squirrels in the UK (Mackinnon 1978). In response to climate warming, there will be no changes in disease dynamics if host species' distributions are simply translated polewards by equal distances without any changes in species' range

overlap. However, both empirical studies (Menendez et al. 2006, Talluto et al. 2017) and mathematical models (Hurford et al. 2019, Zhou and Kot 2011) have shown that in response to climate warming, species lag behind their shifting thermal tolerance limits. These results suggests that for two host species occupying distinct niches along a thermal gradient, the northern species may lag behind its warm tolerance limit in the south as the southern species invades at the northern limit of its range, increasing the area where the two species overlap, thus facilitating disease spread from the northern population to the southern population.

There are many examples of the northward spread of between-host and vector-borne disease in the northern hemisphere, including, malaria (Martens et al. 1996), dengue fever (Hales et al. 2002), bluetongue (Purse et al. 2005), chytrid fungus (Pounds 2001), wooly adelgid beetle in hemlocks (Paradis et al. 2008), beech bark disease (Stephanson et al. 2017), and Lyme disease (Brownstein et al. 2005). There are no examples of southward disease spread in response climate warming in the northern hemisphere, which may be because the conditions for southward spread are more restrictive, given the necessary existence of an isolated susceptible uninfected host population in the south. In addition, some types of pathogen lifecycles may be more amenable to southward disease spread, as southward lags in the pathogen range may be a key feature facilitating the southward spread of disease. Such lags may be likely for diseases with long-lived endotherm hosts (i.e., rabies, bighorn sheep pneumonia, bovine tuberculosis, EHD), and where pathogens with free-living stages which can persist in the environment and survive warm temperatures (e.g., chronic wasting disease).

Testing our hypothesis that climate warming may induce the southward spread of a disease requires a modelling framework that combines reproduction, survival, and dispersal because a lagging species distribution behind a shifting thermal niche is a critical element of facilitating the southward spread of disease. Moving habitat models (Harsch and Zhou 2014) have been formalized as either reaction diffusion equations (Berestyki et al. 2009, Potapov and Lewis 2004), or their discrete time analogue: integrodifference equations (IDEs; Zhou and Kot 2011). Moving habitat models have been used to study how the speed of climate change impacts population dynamics, and how population profiles responds to shifting habitats (Berestyki et al. 2009, Hurford et al. 2019, Potapov and Lewis 2004). Harsch et al. (2017) outlines promising future directions for moving habitat IDE models including incorporating infectious agents and species interactions. To date, IDEs have been used to understand disease dynamics in white pine blister rust (Leung and Kot 2015) and vector-borne mosquito diseases (Kura et al. 2019).

To understand disease dynamics for directly transmitted pathogens in a warming climate, and in a spatially structured host population, we formulate a temperature-driven moving habitat IDE model. We assume that the northern and the southern host populations are identical except for their thermal tolerance limits, and that the landscape consists of a thermal gradient, such that each population occupies a distinct region in the north or in the south. Climate warming shifts the locations of the thermal tolerance limits for both host species northwards, at a constant rate, and equally at all points in space, while all other aspects of the multi-host disease dynamic remain the same. We demonstrate that population densities, when a species' thermal niche is moving due to climate warming, changes the

length of the region of species overlap, particularly due to extinction lags in regions that have become too warm, facilitating the spread of the disease into previously uninfected susceptible southern populations. We discuss rabies in arctic and red foxes, as an example of a population that may demonstrate southward disease spread in response to climate warming.

3.3 Methods

Spatio-temporal dynamics

To describe the spatio-temporal dynamics of disease spread in a warming climate, we use an integrodifference framework (Kot and Schaffer 1986) extended to a system with two epidemiological status:

$$S_{i,t+1}(x) = \int_{-L}^{L}[f_i(S_N, S_S, I_N, I_S, y, t)]k_j(x-y)dy, \quad (1)$$

$$I_{i,t+1}(x) = \int_{-L}^{L}[g_i(S_N, S_S, I_N, I_S, y, t)]k_j(x-y)dy, \quad (2)$$

where $S_{i,t}(y)$ and $I_{i,t}(y)$ is the density of susceptible and infected individuals, respectively, of species *i*, at time *t*, at location *y*, where spatial locations are points on a one-dimensional line, [-L, L], which is understood to correspond to positions along a temperature gradient. The local epidemiological dynamics are described by $f_i(S_{i,t}(y), I_{i,t}(y), r_i(T(y,t))$ and $g_i(S_{i,t}(y), I_{i,t}(y))$, where the former describes the local density of the susceptible individuals after reproduction, mortality, and infection, but prior to dispersal; and the latter describes the local density of infected individuals after infection and mortality, but prior to dispersal. These densities, $f_i(S_{i,t}(y), I_{i,t}(y), r_i(T(y,t))$ and $g_i(S_{i,t}(y), I_{i,t}(y))$, are then multiplied by the probability of dispersal from *y* to *x*,

$$k_j(x-y) = \frac{1}{2D_j} exp^{\frac{-1}{Dj}|x-y|}, \quad (3)$$

which is assumed to follow a Laplace distribution, where the mean dispersal distance, D_j, applies to a specific species-epidemiological status combination, *j*. Integrals in equations

(1) and (2) total the new population density at location *x*, $N_{i,t+1}(x)$, which is comprised of individuals arriving at location *x* from all other locations (*y* in [-L,L]).

Local epidemiological dynamics

We assume a Susceptible-Infected (SI) compartmental framework where infection is lethal such that,

$$f_1(S_N, S_S, I_N, I_S, y, t) = \frac{r_N(T(y,t))S_{N,t}(y)}{1+\frac{(r_N(T(y,t))-1)N_N}{K_N}} - \beta_N S_{N,t}(y)I_{N,t}(y) - \beta_{SN}S_{N,t}(y)I_{S,t}(y), \quad (4)$$

$$f_2(S_N, S_S, I_N, I_S, y, t) = \frac{r_S(T(y,t))S_{S,t}(y)}{1+\frac{(r_S(T(y,t))-1)N_S}{K_S}} - \beta_S S_{S,t}(y)I_{S,t}(y) - \beta_{NS}S_{S,t}(y)I_{N,t}(y), \quad (5)$$

$$g_1(S_N, S_S, I_N, I_S, y, t) = (1 - v)I_{N,t}(y) + \beta_N S_{N,t}(y)I_{N,t}(y) + \beta_{SN}S_{N,t}(y)I_{S,t}(y), \quad (6)$$

$$g_2(S_N, S_S, I_N, I_S, y, t) = (1 - v)I_{S,t}(y) + \beta_S S_{S,t}(y)I_{S,t}(y) + \beta_{NS}S_{S,t}(y)I_{N,t}(y), \quad (7)$$

where,

$$N_N = S_{N,t}(y)+I_{N,t}(y) + \alpha_{SN}(S_{S,t}(y) + I_{S,t}(y)), \quad (8)$$

$$N_S = S_{S,t}(y)+I_{S,t}(y) + \alpha_{NS}(S_{N,t}(y) + I_{N,t}(y)), \quad (9)$$

describe the effective density arising due to competition between the southern and northern species. Species are denoted by the subscripts N representing the northern species and S representing the southern species. Equations (4) and (5) describe the local density of susceptible individuals after local net reproduction, intra- and interspecific competition, and infection. The first term in equations (4) and (5) describes density-dependent net

reproduction and competition following a Beverton-Holt formulation (Beverton and Holt 1957). It is assumed that only susceptible individuals are able to reproduce, but reductions in the net reproductive rate due to density dependence arise due to the presence of both susceptible and infected individuals. The strength of the competitive effect of the southern species on the northern species is represented by the parameter, α_{SN}, and visa versa for the effect of the northern species on the southern species. Each species, has a species-specific carrying capacity, K_i, and a net reproductive rate, $r_i(T(y,t))$ at low densities. Disease transmission occurs via mass action transmission where β_N is the intraspecies transmission rate for the northern species, β_S is the intraspecies transmission rate for southern species, β_{NS} is the interspecies transmission rate from the northern species to the southern species, and β_{SN} is the interspecies transmission rate from the southern species to the northern species.

Equations (6) and (7) describe the local density of infected individuals after infection and mortality, assumes no vertical transmission of infection (i.e., individuals are not born infected). Assumptions regarding the epidemiological dynamics, where chosen to be consistent with arctic rabies, which we later discuss as a disease system in which the southward spread of disease may occur. Due to the assumption of high virulence, the density of infected individuals at the census time, $I_{i,t+1}(x)$, can be low. Therefore, to assess the impact of disease on the population, we also consider the total deaths occurring due to the disease each year, which is simply $R_{t+1}(x) = \int vI_t(y)\, dy$, since the disease is assumed to be lethal.

Temperature, species niches, and climate warming

In equations (4) and (5), species-specific net reproduction at low densities, $r_i(T(y,t))$, is represented as a function of temperature, $T(y,t)$. Specifically, we assume that net reproduction is constant and greater than 1 within the species' thermal tolerance range, and zero outside of the thermal tolerance range, such that,

$$r_i(T(y,t)) = \begin{cases} \rho_i & T_i^{min} < T(y,t) < T_i^{max} \\ 0 & otherwise \end{cases}, \qquad (10)$$

where, T_i^{min} and T_i^{max} are the lowest and highest temperatures, respectively, that species *i* can reproduce and survive at. Notably, we assume that outside the thermal niche, $r_i(T(y,t)) = 0$, and while a more gradual change in the net reproduction rate along the temperature gradient may be more realistic, our assumption of a 'top hat' niche shape represents the least favorable conditions for the northern population to lag behind the southern limit of its thermal tolerance, so as to facilitate the warming-induced spread of the disease into the southern population. Therefore, we expect that if southward disease spread is possible for the 'top hat' niche shape (equation 10), southward disease spread will also occur if niches are assumed to change more continuously as a function of temperature.

Species' thermal tolerance limits translate into hospitable regions due to a relationship between temperature and space, which is assumed to be a linear gradient ranging from T_{max} at $y = -L$ to T_{min} at $y=L$. The assumed effect of climate warming, beginning in year t_{start}, is to increase temperature by w degrees per year at all locations, such that,

$$T(y,t) = \frac{T_{min,i} - T_{max,i}}{2L} + \frac{T_{min,i} + T_{max,i}}{2} + w(t\text{-}t_{start}), \text{ and} \qquad (11)$$

$$w = \begin{cases} 0 & if \quad t < t_{start} \\ > 0 & otherwise \end{cases}$$

In our simulations, each species is given time to disperse into its niche space and reach an equilibrium density prior to the onset of climate change. Climate change is executed as a constant increase in degrees per year, which shifts the niche space a corresponding distance towards the north (x = L).

This model was not parameterized for a specific host-parasite system, rather we used parameters and initial conditions to demonstrate that southward disease spread can occur. We used an initial condition where disease was initially introduced only in the North and parameters were chosen such that, prior to climate change, the species distributions reached an equilibrium where disease was present only in the north, and a southern uninfected population was established (Figure 3.1). We choose our parameters such that the species distributions did not extend beyond the limits of our spatial domain. Our simulations use the same parameter set for both species 1 and 2, with the exception of their thermal tolerance limits (T_i^{min} and T_i^{max}).

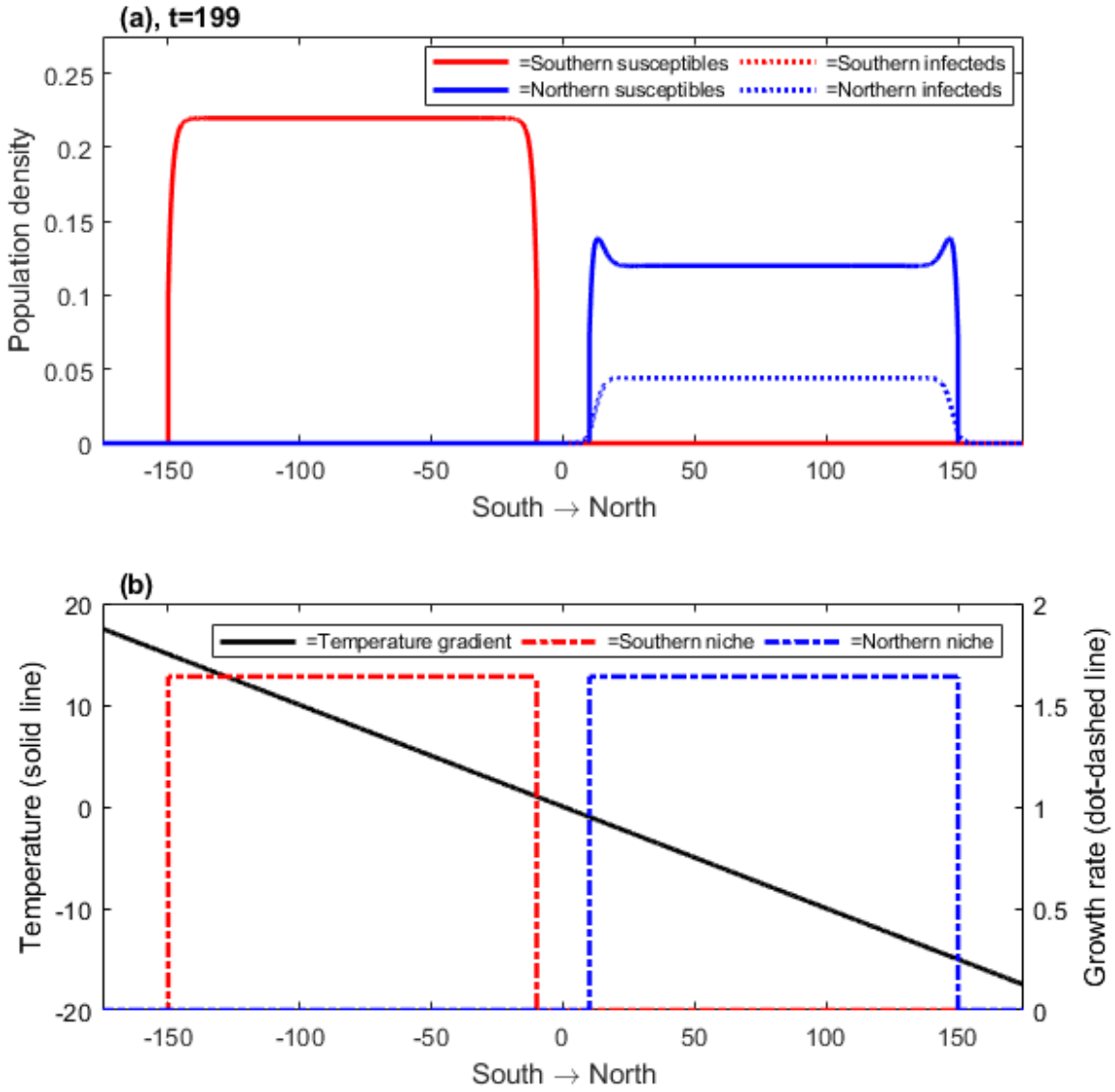

Figure 3.1: Each species has a distinct thermal niche along a temperature gradient with parameters and initial conditions such that the pre-climate change equilibrium population densities have endemic disease in the North only (blue dotted line). Figure 1a shows the southern species (red line) and northern species (blue line) have limited range overlap due to the different temperature limits of their niches and the spatial temperature gradient, and although the southern species is susceptible to the disease, prior to climate warming there is no disease in the southern population (red dotted line) due to the spatial isolation. Figure 1b shows the thermal niche space for the southern (red dash-dotted line) and northern species (blue dash-dotted line). Note that the growth rate for both species is zero outside of their respective niche spaces. The temperature gradient (black line) linearly decreases with latitude and the upper and lower extent of both thermal niches correspond to specific temperature values along that gradient. As climate change occurs, this gradient is uniformly shifted in fixed increments through space.

In order to determine the parameter values that the disease does not spread into the southern population, we ran the simulation without climate change for 300 years (t_{start} > 300) and required that the percent infection prevalence in the southern population was below 0.0001% at the final timestep. Using the same parameter set, we then allowed for climate warming to begin in year t_{start} = 200, which was adequate time for population densities to equilibrate into their niche space. We ran the simulations from time t=0 to time, t=300, with w=0.1 degree per year, therefore, simulating 100 years of climate warming (i.e., 300-t_{start} = 100).

To perform our analyses, we use the fast fourier transform function to numerically calculate the convolution integrals of equations (4-9) and the dispersal kernel (3) in MATLAB 2018a. Computer code is available at: https://doi.org/10.6084/m9.figshare.c.4840686.v1

3.4 Results and Discussion

Our numerical simulations (Figure 3.2) support our hypothesis that climate warming may induce the southward spread of disease, when host species ranges shift northwards. We reason that as climate warming occurs, the northern species lags behind its thermal tolerance limit, which increases the region of overlap between the southern and northern species (Figure 3.3). This lag that facilitates interspecies transmission is also noted in other single species moving habitat models (Berestycki et al. 2009, Zhou and Kot 2011). The increased overlap between the southern and northern host populations is not an assumed consequence of climate warming, but an emergent characteristic of the population and dispersal dynamics in response to a shifting thermal niche. Specifically, as the niche shifts northwards in response to climate warming some individuals do not track with their thermal niches, however, they do not immediately go extinct in habitat which has recently become inhospitable: a phenomenon which has been termed “extinction debt”, and has been demonstrated both empirically (Menendez et al. 2006, Talluto et al. 2017) and theoretically (Hurford et al. 2019, Zhou and Kot 2011).

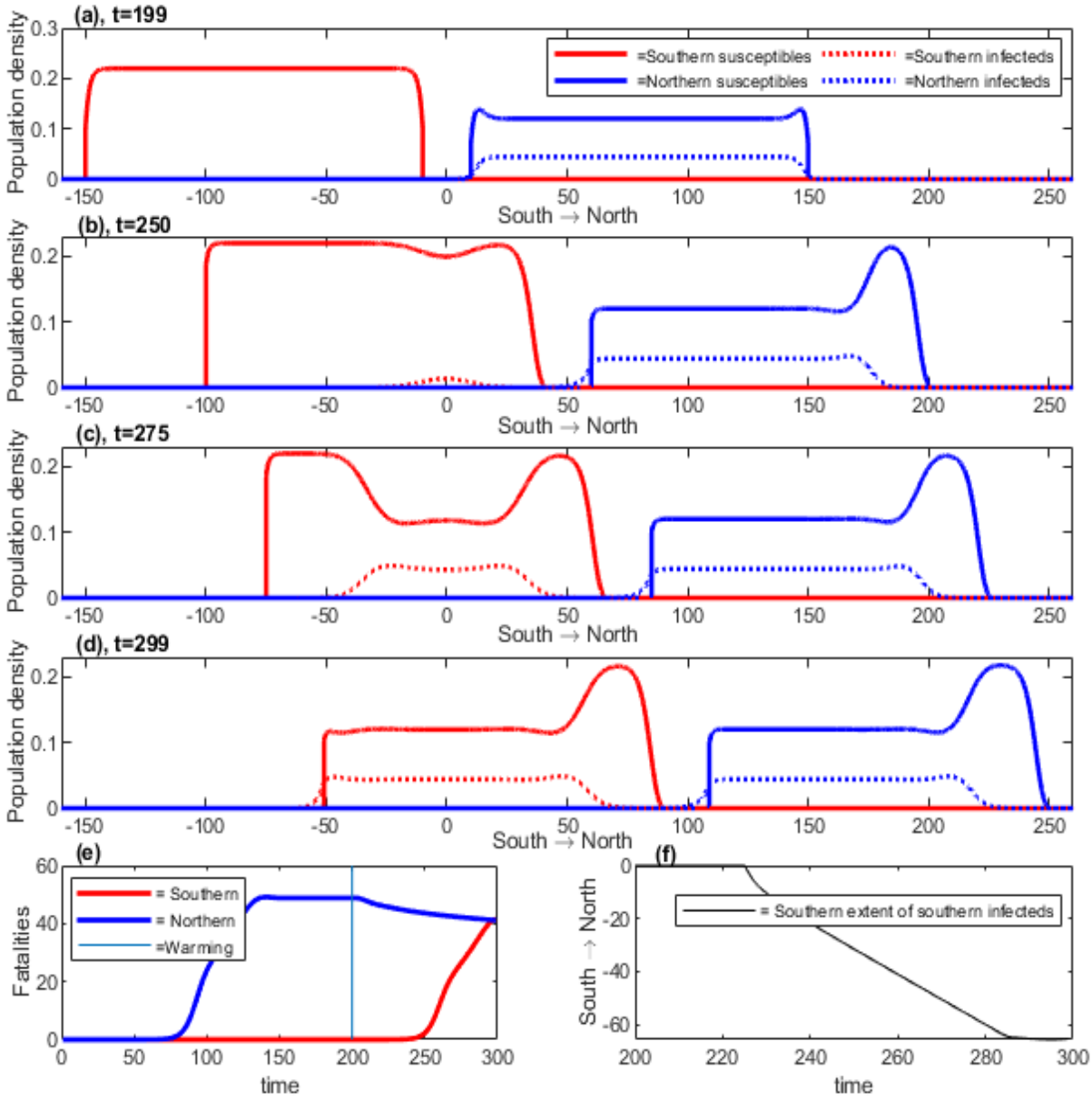

Figure 3.2: Climate warming results in a northern shift in species distributions and southward disease spread. After equilibration of the populations to the densities shown in Figure 3.1 and (a), at t_{start} = 200, a temperature increase of 0.1 degree Celcius per year at every location along the thermal gradient is simulated for a total of 100 years. The densities of susceptible (solid line) and infected (dotted line) individuals for the southern species (red) and northern species (blue) shift northwards as climate warms ((b) t = 250 after 50 years of warming; (c) t=275 after 75 years of warming, and (d) t=299 after 99 years of warming) and disease spreads into the southern population (b,c,d, red dotted line). After climate warming occurs the southern extent of the disease moves southward in space (f). Fatalities per timestep for the southern and northern population are shown in panel (e). Parameters are provided in Table B.1 in Appendix B.

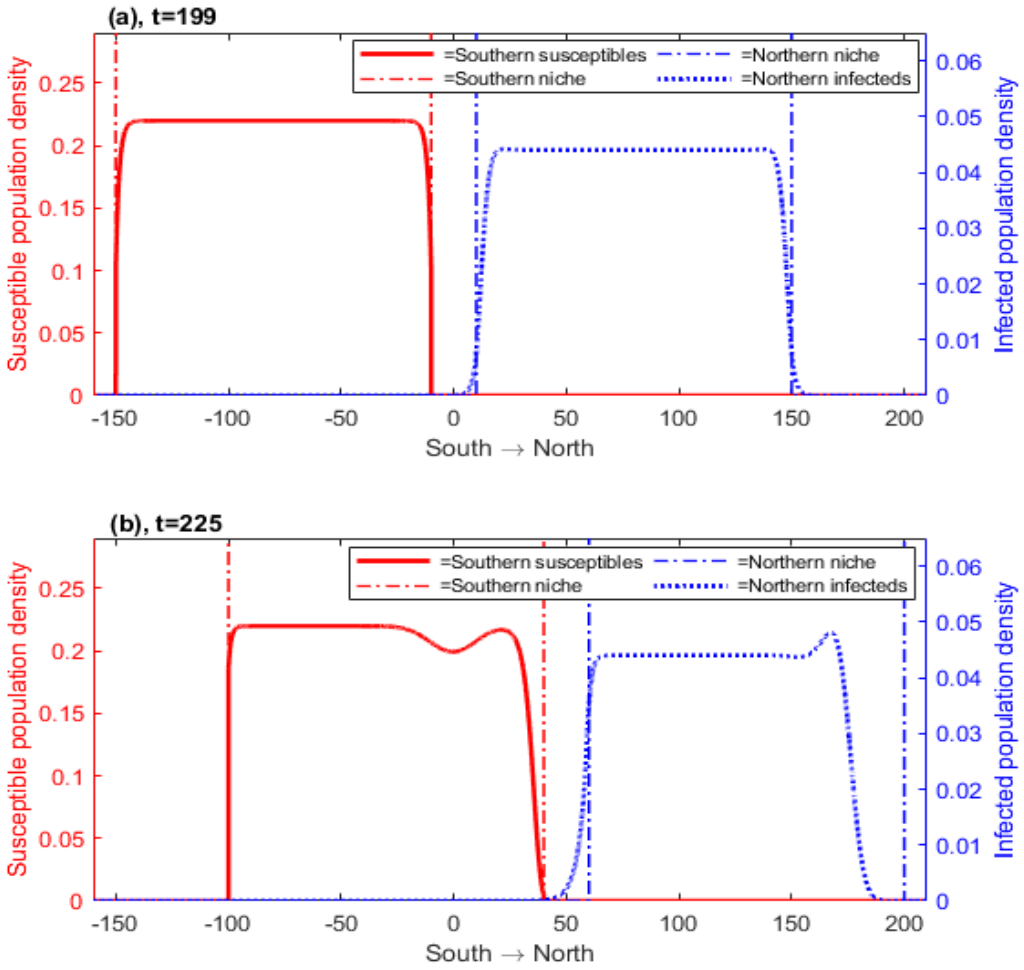

Figure 3.3: When climate warming occurs, lagging northern infecteds "bridge the gap" between previously isolated populations, allowing disease to be transmitted to the uninfected southern population. (a) Prior to climate warming (t=199), the densities of southern susceptibles (solid red line) and northern infecteds (blue dotted line) do not overlap, in part due to the different thermal niches for each population (red and blue dash-dotted lines). (b) After 25 years of continuous climate warming (t=225), the thermal niches of both populations have moved northwards (red and blue dashed-dotted lines), as have the population densities, although often lagging behind the thermal tolerance limits. The lag of the northern infected population (blue dotted line) behind its southern thermal tolerance limit (left-most blue dashed-dotted line) is sufficient to "bridge the gap" to the northern limit of the southern susceptible population (right-most red solid line). The infected northern individuals (blue dashed line) shown south of x = 40 occupy habitat that is too warm at t=225 years (b), and will ultimately go extinct even if no further climate warming occurs; however, extinction takes time and disease spread to the southern population is enabled via this transient persistence. Parameters are as for Figure 3.2 and the density of northern susceptibles and southern infected are not shown to clearly visualize the gap between northern infected and southern susceptibles.

Our result suggests public health implications that may have been previously overlooked, as it is unexpected that northward shifts in host species range may result in the southward spread of disease. However, the conditions required for the southern spread of disease may be restrictive: 1) there must exist a spatially isolated susceptible, but uninfected population in the south (i.e., see Figure 3.1); and 2) the southern population must not be so isolated that it fails to disperse into the regions occupied by the lagging infected northern population made recently suitable for the southern species due to climate warming. Specifically, Figures 3.2 and 3.3 illustrate a parameter space that gives rise to southward spreading disease, even in spite of northward shifting host species ranges, however, not all parameters spaces will yield such a results. Nonetheless, arctic rabies is a disease system exhibiting all the characteristics necessary for warming-induced southward disease spread.

Example: Rabies in red fox and arctic fox

Historically, rabies has been endemic in Arctic fox (the "northern species"), while red foxes (the "southern population") have remained disease-free with only sporadic outbreaks (Mork and Prestrud 2004, Tabel et al 1974). Whether the lack of rabies in red fox populations is the result of stringent vaccination regimes, or different transmission dynamics in southern areas is unclear. The northern range limit of red fox is driven by metabolic requirements and thermal tolerances, while the southern limit of the arctic fox range determined by interspecific competition with red foxes, a superior competitor (Hersteinsson and MacDonald 1992). Currently, the area of overlap for arctic and red fox occurs mainly from the Arctic circle to the southern end of the boreal forest, while some

exceptions occur to the north (i.e. both species are present on Ellesmere Island) (MacPherson 1964, Monchot and Grendon 2010). As climate change occurs, red fox and arctic fox distributions both move northward, and as this occurs, an increase in overlap amongst the two species can be observed in most areas (Gallant et al. 2012, Savory et al. 2014). As such, the arctic rabies system agrees with the formulation of our pre- and post-climate warming scenarios in that prior to climate warming, there exists and uninfected, but susceptible southern population (red fox), and climate warming induces increased overlap between the populations which results facilitates the southward spread of the disease. The epidemiological dynamics we assume (i.e. Susceptible-Infected spread, high virulence and no vertical transmission) are to be consistent with rabies, a lyssavirus known for its high virulence. Rabies has a latent stage that is not considered in our model, however, our timestep of 1 year is 10 to 15 times longer than the latency stage (Anderson et al. 1981, Mork and Prestrud 2004), therefore, we just consider an infectious stage.

The potential for climate warming induced rabies spread into southern regions has implications for rabies that reach beyond the arctic-red fox system. If rabies is spread southward, rabies' disease range will overlap with more host species, specifically bats, skunks, and raccoons (Finnegan et al. 2002), which then presents a threat to these other species via spillover.

We use rabies as a case study for illustration of our southward disease spread scenario, whereby climate warming increases the region of overlap between two host species, however, host-parasite systems where the free-living parasite is long-lived and able to withstand warmer temperatures than the host, are also systems where southward

disease spread may occur. In such systems, if the pathogen is shed, and the climate later warms, the distribution of the pathogen can lag behind the warm tolerance limit of the host. Although many pathogens can persist in the environment for a short period of time (ie., bovine brucellosis; Aune et al. 2012), chronic wasting disease (CWD), spread by infectious prions, can persist for more than 2 years in the environment, and prions from comparable diseases can persist for up to 16 years (Georgsson et al. 2006, Miller et al. 2004). While the spatial incidence of CWD has been fairly random, there are still some areas that are threatened by a southern spread, such as CWD moving southward from Alberta to Montana.

Many studies have been able to show and observe northward shifts in disease as climate warming occurs in the Northern hemisphere (Bellard et al. 2013, Patz et al. 1996, Short et al. 2017), but less studied is the potential for southward disease spread induced by altered contact rates due to climate warming. We show that climate change itself, when paired with temperature dependent niche spaces and spatially structured host populations, can lead to increased disease incidence and prevalence due to spillover into southern populations. There is great potential for moving habitat models to be applied to systems where it is necessary to consider reproduction, survival, competition, and dispersal in multi-host epidemiological systems, providing valuable insight into novel climate-induced spatio-temporal dynamics.

3.5 References

Altizer, S., Ostfeld, R. S., Johnson, P. T., Kutz, S., Harvell, C. D., 2013. Climate change and infectious diseases: from evidence to a predictive framework. science 341, 514-519.

Anderson, R. M., Helen, C. J., Robert, M. M., Anthony, M. S., 1981. Population dynamics of fox rabies in Europe. Nature 289, 765, doi:10.1038/289765a0.

Aune, K., Rhyan, J. C., Russell, R., Roffe, T. J., Corso, B., 2012. Environmental persistence of Brucella abortus in the Greater Yellowstone Area. The Journal of Wildlife Management 76, 253-261.

Bateman, A. W., Neubert, M. G., Krkošek, M., Lewis, M. A., 2015. Generational spreading speed and the dynamics of population range expansion. The American Naturalist 186, 362-375.

Bellard, C., Thuiller, W., Leroy, B., Genovesi, P., Bakkenes, M., Courchamp, F., 2013. Will climate change promote future invasions? Global Change Biology 19, 3740-3748.

Berestycki, H., Diekmann, O., Nagelkerke, C. J., Zegeling, P. A., 2009. Can a species keep pace with a shifting climate? Bulletin of mathematical biology 71, 399.

Beverton, R. J. Holt., 1957. On the dynamics of exploited fish populations. London, H. M. Stationery Off., London.

Brownstein, J. S., Holford, T. R., Fish, D., 2005. Effect of climate change on lyme disease risk in North America. EcoHealth 2, 38-46, doi:10.1007/s10393-004-0139-x.

Chen, I. C., Hill, J. K., Ohlemüller, R., Roy, D. B., Thomas, C. D., 2011. Rapid range shifts of species associated with high levels of climate warming. Science 333, 1024, doi:10.1126/science.1206432.

Finnegan, C. J., Brookes, S. M., Johnson, N., Smith, J., Mansfield, K. L., Keene, V. L., McElhinney, L. M., Fooks, A. R., 2002. Rabies in North America and Europe. Journal of the Royal Society of Medicine 95, 9-13.

Gallant, D., Slough, B. G., Reid, D. G., Berteaux, D., 2012. Arctic fox versus red fox in the warming Arctic: four decades of den surveys in north Yukon. Polar Biology 35, 1421-1431, doi:10.1007/s00300-012-1181-8.

Georgsson, G., Sigurdarson, S., Brown, P., 2006. Infectious agent of sheep scrapie may persist in the environment for at least 16 years. Journal of General Virology 87, 3737-3740.

Hales, S., de Wet, N., Maindonald, J., Woodward, A., 2002. Potential effect of population and climate changes on global distribution of dengue fever: an empirical model. The Lancet 360, 830-834, doi:https://doi.org/10.1016/S0140-6736(02)09964-6.

Harsch, M. A., Zhou, Y., Hillerislambers, J., Kot, M., 2014. Keeping pace with climate change: stage-structured moving-habitat models. The American Naturalist 184, 25-37.

Harsch, M. A., Phillips, A., Zhou, Y., Leung, M. R., Rinnan, D. S., Kot, M., 2017. Moving forward: insights and applications of moving-habitat models for climate change ecology. Journal of Ecology 105, 1169-1181.

Harvell, C. D., Mitchell, C. E., Ward, J. R., Altizer, S., Dobson, A. P., Ostfeld, R. S., Samuel, M. D., 2002. Climate warming and disease risks for terrestrial and marine biota. Science 296, 2158-2162.

Hersteinsson, P., MacDonald, D. W., 1992. Interspecific competition and the geographical distribution of red and arctic foxes Vulpes vulpes and Vulpes lagopus. Oikos 64, 505-515, doi:10.2307/3545168.

Hurford, A., Cobbold, C. A., Molnár, P. K., 2019. Skewed temperature dependence affects range and abundance in a warming world. bioRxiv, 408104.

Houghton, J. T., Ding, Y., Griggs, D. J., Noguer, M., van der Linden, P. J., Dai, X., Maskell, K., Johnson, C., 2001. Climate change 2001: the scientific basis. The Press Syndicate of the University of Cambridge.

Kim, B. I., Blanton, J. D., Gilbert, A., Castrodale, L., Hueffer, K., Slate, D., Rupprecht, C. E., 2014. A conceptual model for the impact of climate change on fox rabies in Alaska, 1980–2010. Zoonoses and public health 61, 72-80.

Kura, K., Khamis, D., El Mouden, C., Bonsall, M., 2019. Optimal control for disease vector management in SIT models: an integrodifference equation approach. Journal of Mathematical Biology 78, 1821-1839.

Leung, M. R., Kot, M., 2015. Models for the spread of white pine blister rust. Journal of Theoretical Biology 382, 328-336.

MacKinnon, K., 1978. Competition between red and grey squirrels. Mammal Review 8, 185-190.

MacPherson, A. H., 1964. A northward range extension of the red fox in the eastern canadian arctic. Journal of Mammalogy 45, 138-140, doi:10.2307/1377304.

Martens, W. J., Niessen, L. W., Rotmans, J., Jetten, T. H., McMichael, A. J., 1995. Potential impact of global climate change on malaria risk. Environmental health perspectives 103, 458-464, doi:10.1289/ehp.95103458.

Menéndez, R., Megías, A. G., Hill, J. K., Braschler, B., Willis, S. G., Collingham, Y., Fox, R., Roy, D. B., Thomas, C. D., 2006. Species richness changes lag behind climate change. Proceedings of the Royal Society B: Biological Sciences 273, 1465-1470.

Miller, M. W., Williams, E. S., Hobbs, N. T., Wolfe, L. L., 2004. Environmental sources of prion transmission in mule deer. Emerging infectious diseases 10, 1003.

Molnár, P. K., Derocher, A. E., Thiemann, G. W., Lewis, M. A., 2010. Predicting survival, reproduction and abundance of polar bears under climate change. Biological Conservation 143, 1612-1622, doi:https://doi.org/10.1016/j.biocon.2010.04.004.

Molnár, P. K., Kutz, S. J., Hoar, B. M., Dobson, A. P., 2013. Metabolic approaches to understanding climate change impacts on seasonal host-macroparasite dynamics. Ecology Letters 16, 9-21.

Monchot, H., Gendron, D., 2010. Disentangling long bones of foxes (Vulpes vulpes and Alopex lagopus) from arctic archaeological sites. Journal of Archaeological Science 37, 799-806, doi:10.1016/j.jas.2009.11.009.

Moorcroft, P. R., Pacala, S., Lewis, M., 2006. Potential role of natural enemies during tree range expansions following climate change. Journal of Theoretical Biology 241, 601-616.

Mørk, T., Prestrud, P., 2004. Arctic Rabies – A Review. Acta Veterinaria Scandinavica 45, 1, doi:10.1186/1751-0147-45-1.

Neubert, M. G., Caswell, H., 2000. Demography and dispersal: calculation and sensitivity analysis of invasion speed for structured populations. Ecology 81, 1613-1628.

Paradis, A., Elkinton, J., Hayhoe, K., Buonaccorsi, J., 2008. Role of winter temperature and climate change on the survival and future range expansion of the hemlock woolly adelgid (Adelges tsugae) in eastern North America. Mitigation and Adaptation Strategies for Global Change 13, 541-554, doi:10.1007/s11027-007-9127-0.

Parkinson, A. J., Butler, J. C., 2005. Potential impacts of climate change on infectious diseases in the Arctic. International Journal of Circumpolar Health 64, 478-486, doi:10.3402/ijch.v64i5.18029.

Patz, J. A., Epstein, P. R., Burke, T. A., Balbus, J. M., 1996. Global climate change and emerging infectious diseases. JAMA 275, 217-223, doi:10.1001/jama.1996.03530270057032.

Potapov, A. B., Lewis, M. A., 2004. Climate and competition: the effect of moving range boundaries on habitat invasibility. Bulletin of mathematical biology 66, 975-1008.

Pounds, J. A., 2001. Climate and amphibian declines. Nature 410, 639, doi:10.1038/35070683.

Purse, B. V., Mellor, P. S., Rogers, D. J., Samuel, A. R., Mertens, P. P. C., Baylis, M., 2005. Climate change and the recent emergence of bluetongue in Europe. Nature reviews. Microbiology 3, 171-181.

Savory, G. A., Hunter, C. M., Wooller, M. J., O'Brien, D. M., 2014. Anthropogenic food use and diet overlap between red foxes (Vulpes vulpes) and arctic foxes (Vulpes lagopus) in Prudhoe Bay, Alaska. Canadian Journal of Zoology 92, 657-663, doi:10.1139/cjz-2013-0283.

Short, E. E., Caminade, C., Thomas, B. N., 2017. Climate change contribution to the emergence or re-emergence of parasitic diseases. Infectious diseases 10, 1178633617732296-1178633617732296, doi:10.1177/1178633617732296.

Stephanson, C., Coe, N., 2017. Impacts of beech bark disease and climate change on American Beech. Forests 8, 155, doi:10.3390/f8050155.

Tabel, H., Corner, A. H., Webster, W. A., Casey, C. A., 1974. History and epizootiology of rabies in Canada. Can Vet J 15.

Talluto, M. V., Boulangeat, I., Vissault, S., Thuiller, W., Gravel, D., 2017. Extinction debt and colonization credit delay range shifts of eastern North American trees. Nature Ecology & Evolution 1, 0182.

Trewhella, W. J., Harris, S., McAllister, F. E., 1988. Dispersal distance, home-range size and population density in the red fox (Vulpes vulpes): A Quantitative Analysis. Journal of Applied Ecology 25, 423-434, doi:10.2307/2403834.

Urban, M. C., Zarnetske, P. L., Skelly, D. K., 2013. Moving forward: dispersal and species interactions determine biotic responses to climate change. Annals of the New York Academy of Sciences 1297, 44-60.

Zhou, Y., Kot, M., 2011. Discrete-time growth-dispersal models with shifting species ranges Theoretical Ecology 4, 13-25.

Zhou, Y., Kot, M., 2013. Life on the move: modeling the effects of climate-driven range shifts with integrodifference equations. Dispersal, individual movement and spatial ecology. Springer, pp. 263-292.

Chapter 4: Conclusion and Summary

Arctic rabies is a complex system with many unanswered questions. These questions come in the form of discrepancies between observed disease dynamics and those produced by mathematical models, in addition to the potential quantitative and qualitative shifts that a warming climate will likely induce. Arctic rabies is also unique in that it occurs in largely undeveloped areas of the world where research is difficult to coordinate and conduct. This leaves mathematical modeling as a powerful tool to understand, predict, and test rabies driven hypotheses. Despite this, there are few studies that explore the paradox between rabies persistence and the low densities that should not be able to maintain the disease, with Simon et al. (2019) being one of the foundational studies in which we worked forward from. Once we are able to understand what maintains rabies, we are still left with the question of what will become of it, given climate induced range shifts.

To answer our first question, we were able to contextualize arctic rabies via developed metapopulation theory concepts in chapter 2. Contrary to theoretical calculations that report a critical density (K_T) of approximately 1 fox/km^2 for rabies endemicity, arctic rabies persists at densities well below this (Anderson et al. 1981, Simon et al. 2019). The calculation of K_T = 1 fox/km^2 assumes a uniform fox density across the landscape and unrestricted mixing between susceptible and infected foxes. We hypothesized that spatial heterogeneity, arising from resource distribution or social structure, may result in regions where rabies is endemic, even though average fox densities at the landscape-level are below K_T. To expand on research investigating the persistence of arctic rabies, we examined arctic rabies via a two-patch structure. We found that rabies

can persist in a heterogeneous landscape, where the mean carrying capacity is below the threshold carrying capacity required for endemicity in a homogeneous landscape. Rabies endemicity in low-carrying capacity regions within heterogeneous landscapes is facilitated by high transmission rates, potentially due to 'floater' foxes; and when only latently-infected or infected foxes move between patches. Our results suggest that rabies may persist in heterogeneous landscapes when the mean landscape-level carrying capacity is as low as ~0.25 foxes/km^2 and on sink patches with densities as low as 0.036 foxes/km^2.

While our two-patch model was a useful simplification to study arctic rabies, there is still more research to be completed in order to fully apply metapopulation theory to arctic rabies. This includes delineating the scale at which foxes interact, both in terms of population dynamics (e.g. dispersal rates, genetic connectivity) and epidemic dynamics (e.g. the correlation of outbreaks across space), which would allow for a more thorough understanding of what a metapopulation structure denotes in fox populations. Other useful research could include a more detailed measurement of source populations, such as the densities around resource rich areas, and the connectivity of those areas to "sinks'. With that information, a metapopulation model would be able to be parametrized with much more precision than the parameter estimation used in this model.

To answer our second question, we applied a moving habitat model to a multispecies disease system, which reflected the qualitative features of arctic rabies amongst its main host, arctic foxes, and its secondary host to the south, red foxes. Poleward movement of wildlife ranges and their corresponding diseases is supported by countless observations, empirical measurements, and predictions that explore a species' response to

a warming climate (Bellard et al. 2013, Patz et al. 1996, Short et al. 2017). We considered an alternative scenario whereby disease moves southward rather than northward in response to climate induced range shifts. This is particularly relevant to viral, bacterial, and prion diseases that do not have thermal tolerance limits and are inextricably linked to their hosts distribution. We formulated a moving habitat integrodifference model with a Susceptible-Infected epidemiological structure for two competing species with different temperature-dependent niche spaces. We presented a scenario in which climate change facilitates disease movement southward through space as climate warming moves our niche space northward. Our results show that there is a counterintuitive scenario in which southern species may see an increase risk for disease outbreaks and incidence in response to climate change. We explored this in the context of rabies in arctic and red fox, and note the potential for southward spread and further spillover to additional hosts as the disease moves south, presenting an increasing zoonotic threat.

Our third chapter was one of the primary attempts in the literature to understand disease dynamics in moving habitat models (Harsch et al. (2017) investigates SI disease dynamics in a single species moving habitat model, Leung and Kot (2015) investigate white pine blister rust, and Kura et al. (2019) investigate vector-borne mosquito diseases). We note the effects that using a rectangular niche space created, such as our need to definitively separate the two species' thermal niche spaces in our primary simulation. The logical next step would be formulating a niche space based on a skew or standard distribution. This would address our assumption that for disease to be isolated prior to climate change, the populations must either be distinctly separate, or an alternative

assumption whereby one of the populations must transmit the disease far less than the other, and interspecies transmission must be reduced. By relaxing these assumption, it is likely that one could study disease dynamics in a moving habitat model where an endemically infected population has minor overlap with a disease free population, when both populations exhibit the same epidemiological characteristics.

We were able to use developed modeling techniques to understand an epidemiological system that is not well understood. We were able to show that rabies can, in fact, persist in the low carrying capacities of the Arctic, and we were able to test the robustness of these results to assumptions based on mobility (i.e. floaters) and selective dispersal. We also simulated potential disease dynamics that may occur in a warming world; highlighting a counterintuitive scenario whereby disease will move southward. For wildlife managers, our results suggest that identification of disease sources, which are critical to the maintenance of rabies in the Arctic, may be the key to successful oral vaccination regimes for disease management and elimination. Our results will also clarify disease dynamics, should a southern wave of rabies arise; and our results delineate the transient area of overlap between two species undergoing climate induced range shift as the site of spillover and potential disease suppression via vaccination. With this research, I hope that I can contribute, and help others move towards a deeper understanding of rabies in the Arctic.

4.1 References

Anderson, R. M., Helen, C. J., Robert, M. M., Anthony, M. S., 1981. Population dynamics of fox rabies in Europe. Nature 289, 765, doi:10.1038/289765a0.

Bellard, C., Thuiller, W., Leroy, B., Genovesi, P., Bakkenes, M., Courchamp, F., 2013. Will climate change promote future invasions? Global Change Biology 19, 3740-3748.

Harsch, M. A., Phillips, A., Zhou, Y., Leung, M. R., Rinnan, D. S., Kot, M., 2017. Moving forward: insights and applications of moving-habitat models for climate change ecology. Journal of Ecology 105, 1169-1181.

Kura, K., Khamis, D., El Mouden, C., Bonsall, M., 2019. Optimal control for disease vector management in SIT models: an integrodifference equation approach. Journal of Mathematical Biology 78, 1821-1839.

Leung, M. R., Kot, M., 2015. Models for the spread of white pine blister rust. Journal of Theoretical Biology 382, 328-336.

Patz, J. A., Epstein, P. R., Burke, T. A., Balbus, J. M., 1996. Global climate change and emerging infectious diseases. JAMA 275, 217-223, doi:10.1001/jama.1996.03530270057032.

Short, E. E., Caminade, C., Thomas, B. N., 2017. Climate Change Contribution to the Emergence or Re-Emergence of Parasitic Diseases. Infectious diseases 10, 1178633617732296-1178633617732296, doi:10.1177/1178633617732296.

Simon, A., Tardy, O., Hurford, A., Lecomte, N., Bélanger, D., Leighton, P., 2019. Dynamics and persistence of rabies in the Arctic. Polar Research, 38 https://doi.org/10.33265/polar.v38.3366

Appendix A

A.1 Selective dispersal model

The following model is a modified version of the previously stated two-patch model in chapter 2. In addition to our prior formulation, each equation here has 2 additional terms. The general dispersal from patch to patch, m_{12} and m_{21} have been modified to ms_{12}, me_{12}, mi_{12}, and ms_{21}, me_{21}, mi_{21}. The addition of the s, e, and i to each dispersal term represents the epidemiological compartment that is dispersing. This formulation allowed us to selectively disperse foxes of different disease statuses.

$$\dot{S}_1 = rS_1 - \mu_1 S_1 N_1 - \beta S_1 I_1 - S_1 m_{12} - S_1 ms_{12} + S_2 m_{21} + S_2 ms_{21} \quad (1)$$

$$\dot{E}_1 = \beta S_1 I_1 - E_1(p+d) - \mu_1 E_1 N_1 - E_1 m_{12} - E_1 me_{12} + E_2 m_{21} + E_2 me_{21} \quad (2)$$

$$\dot{I}_1 = pE_1 - I_1(v+d) - \mu_1 I_1 N_1 - I_1 m_{12} - I_1 mi_{12} + I_2 m_{21} + I_2 mi_{21} \quad (3)$$

$$\dot{S}_2 = rS_2 - \mu_2 S_2 N_2 - \beta S_2 I_2 - S_2 m_{21} - S_2 ms_{21} + S_2 m_{12} + S_2 ms_{12} \quad (4)$$

$$\dot{E}_2 = \beta S_2 I_2 - E_2(\rho+d) - \mu_2 E_2 N_2 - E_2 m_{21} - E_2 me_{21} + E_2 m_{12} + E_2 me_{12} \quad (5)$$

$$\dot{I}_2 = \rho E_2 - I_2(v+d) - \mu_2 I_2 N_2 - I_2 m_{21} - I_2 mi_{21} + I_2 m_{12} + I_2 mi_{12} \quad (6)$$

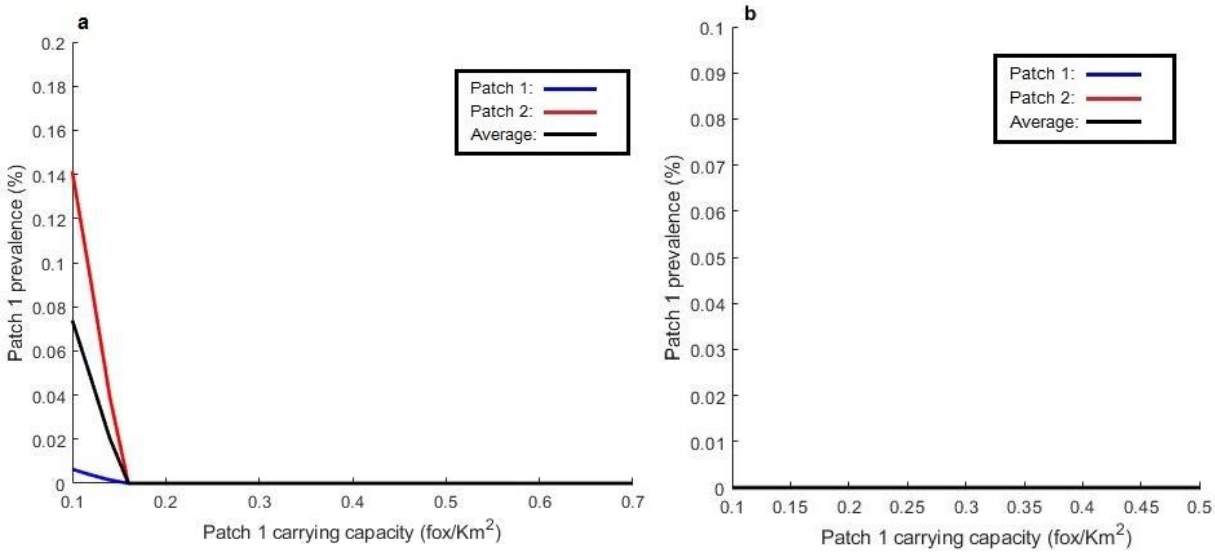

Figure A.1: Very low landscape level averages $\overline{K}$=0.7 fox/km^2 (a) and $\overline{K}$=0.5 fox/km^2 (b) provide limited parameter space for endemicity (a) and can be exhausted of its disease by dispersal without effectively infecting the other patch (b). $\overline{K} = (K_1 + K_2)/2$, is taken across the two patches in the landscape. The landscape-level prevalence (%) of rabies, is for ascending values of the low-carrying capacity patch 1, and the carrying capacity on patch 2 is $2\overline{K} - K_1$. When $K_1 = K_2 = \overline{K}/2 < K_T$, no disease occurs on either patch, however, as the variance in the K_i between the two patches increases, rabies becomes established on both patches in (a), although at extremely low prevalence. Dispersal is unidirectional with m_{12}=0 and m_{21}=0.1. Unless otherwise stated, all parameter values are as given in Table 2.1.

A.2 Blackwood formulation and floater model

This model uses the same formulation as the equations presented in chapter 2, with the exception of the transmission term, which is further discussed here.

Blackwood formulation: $\beta S(I + \varphi)$ where the parameter φ represents the additive disease effect from floaters. This model assumes that when the infected animals on a patch go to zero, the floaters (ie. φ) continues to infect the population. Therefore, when disease dynamics lead to a fade out or burnout, the equilibrium prevalence of a population is proportional to φ. New infections are transmitted from floaters in every timestep, regardless of the population dynamics of residents, forcing an unstable disease free equilibrium (Brauer and van den Driessche 2001).

Our formulation: $(\beta \cdot b_f)(I \cdot fp)S$, where b_f and fp are parameters that represent the efficacy of floater transmission relative to residents, and the proportion of infected floaters relative to residents. With this modification, we are able to elevate the population level transmission coefficient to account for floater-driven interactions. Although this model includes higher mobility through an additive infection term, we multiply the additive effect of floaters by the resident population, therefore, when S or I go to zero, so do the effects of floaters. This allows us to relax the assumptions of Blackwood et al. (2013) and Simon et al. (2019) that if the infected population on a patch goes extinct, then floaters can still infect the resident population by reemerging at every timestep in a proportion equal to φ. Because of this assumption, the Blackwood formulation forces an unstable disease-free equilibrium because new infections are transmitted from floaters in every timestep, regardless of

resident population dynamics, specifically $K<K_T$. This formulation is not seen in the paper, as we just report the beta values that result from this multiplication.

A.3 References - Appendix A

Blackwood, J. C., Streicker, D. G., Altizer, S., Rohani, P., 2013. Resolving the roles of immunity, pathogenesis, and immigration for rabies persistence in vampire bats. Proceedings of the National Academy of Sciences of the Unites States of America 110, 20837-20842.

Brauer, F., van den Driessche, P., 2001. Models for transmission of disease with immigration of infectives. Mathematical Biosciences 171, 143-154, doi:https://doi.org/10.1016/S0025-5564(01)00057-8.

Simon, A., Tardy, O., Hurford, A., Lecomte, N., Bélanger, D., Leighton, P., 2019. Dynamics and persistence of rabies in the Arctic. Polar Research 38. https://doi.org/10.33265/polar.v38.3366

Appendix B

Table B.1: Parameter descriptions for the SI integrodifference model (equations 3-11). Subscripts denote patch specific values. The parameter values are the same for each species, with the exception of their thermal tolerance range.

Definition	***Parameter***	***Value***
Northern species carrying capacity	K_N	6 individuals/space
Southern species carrying capacity	K_S	6 individuals/space
Northern species growth rate	r_N	1.64 yr^{-1}
Southern species growth rate	r_S	1.64 yr^{-1}
Northern species dispersal rate	D_N	1 yr^{-1}
Southern species dispersal rate	D_S	1 yr^{-1}
Competitive effect of northern species on southern species	α_{NS}	0.25 yr^{-1}
Competitive effect of southern species on northern species	α_{SN}	0.25 yr^{-1}
Northern species transmission coefficient	B_N	2.5 space/year/individual
Southern species transmission coefficient	B_S	2.5 space/year/individual
Virulence	v	0.3 yr^{-1}
Southern species lower thermal tolerance	T_S^{min}	1°C
Southern species upper thermal tolerance	T_S^{max}	15°C
Northern species lower thermal tolerance	T_N^{min}	-15°C
Northern species upper thermal tolerance	T_N^{max}	-1°C
Temperature gradient	c	0.1°C